NACA RM L52D17a

NACA

RESEARCH MEMORANDUM

EFFECTS OF SEVERAL HIGH-LIFT AND STALL-CONTROL DEVICES ON THE AERODYNAMIC CHARACTERISTICS OF A SEMISPAN 49° SWEPTBACK WING

By U. Reed Barnett, Jr., and Stanley Lipson

Langley Aeronautical Laboratory
Langley Field, Va.

NATIONAL ADVISORY COMMITTEE FOR AERONAUTICS

WASHINGTON

September 15, 1952

NATIONAL ADVISORY COMMITTEE FOR AERONAUTICS

RESEARCH MEMORANDUM

EFFECTS OF SEVERAL HIGH-LIFT AND STALL-CONTROL DEVICES ON THE AERODYNAMIC CHARACTERISTICS OF A SEMISPAN 49° SWEPTBACK WING

By U. Reed Barnett, Jr., and Stanley Lipson

SUMMARY

A low-speed investigation has been conducted in the Langley full-scale tunnel to determine the effects of several high-lift and stall-control devices on the aerodynamic characteristics of a semispan wing with 49.1° sweepback of the leading edge. The model had an aspect ratio of 3.78, a taper ratio of 0.586, and incorporated NACA 65A006 airfoil sections streamwise. The devices investigated were a leading-edge extensible flap, a slat, a plain trailing-edge flap, and a fence. Limited tests were also conducted of boundary-layer control by blowing over the trailing-edge flap and by suction through a spanwise slot. Rolling characteristics of a flap-type aileron were obtained for both the basic wing and the wing equipped with stall-control devices. All tests were conducted at a Reynolds number of 6.1×10^6, except for the blowing tests which were made at a Reynolds number of 4.4×10^6.

At zero angle of attack, the plain trailing-edge flap produced an increment in lift coefficient of 0.36 at a flap deflection of 60°, but it was relatively ineffective in increasing the maximum lift. Because of the limited quantity of air employed in this preliminary test, only small lift gains were realized as a result of blowing air over the deflected trailing-edge flap.

The use of either the 0.5-wing-semispan leading-edge flap or slat, with the trailing-edge flap neutral, resulted in a reduction of the severity of the unstable break from that obtained with the basic wing. The slat appears to be somewhat more effective than the leading-edge flap in improving the effectiveness of the aileron in the high angle-of-attack range.

In the high lift range, the best lift-to-drag ratio was obtained with the trailing-edge flap deflected 45° and either the leading-edge flap or slat installed.

INTRODUCTION

As part of a general investigation by the National Advisory Committee for Aeronautics to study, at large scale, the effectiveness of various stall-control and high-lift devices towards improving the low-speed characteristics of high-speed wing plan forms, tests were conducted in the Langley full-scale tunnel to determine the longitudinal aerodynamic characteristics of a semispan 49.1° sweptback wing. The wing incorporated NACA 65A006 sections streamwise and had an aspect ratio of 3.78 and a taper ratio of 0.586. Presented in this paper are the results of tests of a leading-edge extensible flap, a slat, and a plain trailing-edge flap. In addition, the effect of the stall-control devices on the rolling-moment characteristics of a flap-type aileron are also presented. The results of the basic wing tests and of tests varying the slat span and deflection angle are reported in reference 1.

In addition to the flap studies, a preliminary investigation was conducted to determine the effect on the stalling and maximum-lift characteristics of the wing of boundary-layer suction through a spanwise slot located on the upper surface of the wing, and of blowing a high-velocity jet of air over the deflected trailing-edge flap.

All tests were conducted at a Reynolds number of 6.1×10^6 and a Mach number of 0.10, except for the blowing tests which were made at a Reynolds number of 4.4×10^6 and a Mach number of 0.07.

COEFFICIENTS AND SYMBOLS

The data are referred to the wind axes with the origin at the quarter-chord point of the mean aerodynamic chord. The data have been reduced to standard NACA nondimensional coefficients which are defined as follows:

C_L lift coefficient, $\dfrac{\text{Twice model lift}}{qS}$

$C_{L_{max}}$ maximum lift coefficient

C_D drag coefficient, $\dfrac{\text{Twice model drag}}{qS}$

C_m pitching-moment coefficient about quarter-chord point of mean aerodynamic chord, $\dfrac{\text{Twice model pitching moment}}{qS\bar{c}}$

[redacted]

C_l rolling-moment coefficient, $\frac{\text{Rolling moment}}{qSb}$

C_p pressure coefficient, $\frac{H - H_d}{q}$

C_Q flow coefficient, $\frac{Q}{VS'}$

R Reynolds number, $\frac{\rho}{\mu}V\bar{c}$

H free-stream total pressure, lb/ft^2

H_d total pressure inside wing duct, lb/ft^2

q free-stream dynamic pressure, $\frac{\rho}{2}V^2$, lb/ft^2

Q twice quantity of air used in boundary-layer control tests, ft^3/sec

S twice area of semispan wing, ft^2

S' twice model wing area affected by boundary-layer control, ft^2

$\bar{c}$ mean aerodynamic chord, $\frac{2}{S}\int_0^{b/2} c^2 dy$, ft

ρ mass density of air, $slugs/ft^3$

V free-stream velocity, ft/sec

μ coefficient of viscosity, slugs/ft-sec

c local wing chord measured parallel to plane of symmetry, ft

c' local wing chord measured perpendicular to 0.50c' line, ft (see fig. 1)

c_f' local flap chord measured perpendicular to 0.50c' line, ft (see fig. 1)

c_s' local slat chord measured perpendicular to 0.50c' line, ft (see fig. 1)

b twice span of semispan wing, ft

[redacted]

α	angle of attack, deg
δ_f	trailing-edge-flap deflection angle, deg
δ_a	aileron deflection angle, deg
$\Delta C_{L_{max}}$	increment in maximum lift coefficient

MODEL

The semispan wing is shown mounted on a reflection plane in the Langley full-scale tunnel in figure 2. A description of the reflection plane is presented in reference 2. The geometric characteristics and principal dimensions of the semispan wing are given in figure 1. The wing has 49.1° of sweepback at the leading edge, an aspect ratio of 3.78, a taper ratio of 0.586, and no geometric dihedral or twist. The airfoil section parallel to the air stream is an NACA 65A006 section. The wing tip is half of a body of revolution based on the same airfoil section ordinates.

The high-lift and stall-control devices (figs. 1 and 3) employed were: 0.15c' leading-edge slat installed at the outboard 50 percent of the wing semispan; a 0.10c' leading-edge flap also tested at the outboard $0.50\frac{b}{2}$ location; a 0.25c' inboard trailing-edge flap having a span of $0.469\frac{b}{2}$; and a chordwise fence having a height of 0.036c, based on the midsemispan chord, and divided into four separate sections. The fence, which was made of $\frac{1}{4}$-inch plywood, was mounted parallel to the free-stream direction. The nose and upper surface of the slat have the ordinates of the wing airfoil but the slat is not an integral part of the wing and is mounted directly onto the unmodified basic wing leading edge with the slat brackets alined normal to the leading edge of the wing. Further details of the slat arrangement may be obtained from reference 1. The leading-edge flap is made of sheet metal welded to a 1.375-inch-diameter steel tube.

In addition to the devices previously described, the wing is equipped with two spanwise slots for boundary-layer control. A spanwise slot, 0.01c' wide, is located at 0.20c' on the upper surface of the wing (fig. 1) and is employed for boundary-layer control by suction. The lip shape and entrance angle are illustrated in figure 3 and duplicate those used in the investigation reported in reference 3. Immediately ahead of the trailing-edge flap is the second slot which opens into

the upper portion of the gap between the airfoil and the flap and is used for blowing air over the flap. The slot gap employed was a $\frac{1}{2}$-inch opening along the entire flap span and represents an 0.00425c gap when based on the average streamwise chord for that portion of the wing which contains the blowing slot. The slots are connected to a blower by ducts inside the wing which extend through the reflection plane at the wing root. Flexible ducting was used beneath the reflection plane to connect the wing ducts to the stationary blower ducts in such a manner as to minimize the force transmitted from the blower ducts to the balance system. All slots were sealed with wooden blocks and smoothly faired to the wing contour when not in use.

For the aileron tests, a flap-type aileron, having a chord length of 0.25c' and divided into two spanwise sections, was used. The inboard aileron began at $0.61\frac{b}{2}$, which was immediately outboard of the flap, and had a span of $0.234\frac{b}{2}$, while the outboard aileron had a span of $0.156\frac{b}{2}$ and extended to the wing tip (fig. 1). The chord profile of the aileron was the same as that of the flap. Both the trailing-edge flap and the aileron were hinged normal to the 0.50c' line.

TESTS AND CORRECTIONS

Description of tests.- Data were obtained through an angle-of-attack range from approximately -2° to 31°. Force measurements were made to determine the lift, pitching-moment, and drag characteristics of the basic wing alone and in various combinations with the high-lift and stall-control devices. The rolling-moment characteristics of the aileron were determined for the basic wing and for the wing with stall-control devices. All tests, except the blowing tests, were made at a Reynolds number of 6.1×10^6 and a Mach number of 0.10. For the blowing tests the Reynolds number was 4.4×10^6 and the Mach number was 0.07.

Only a limited number of boundary-layer-control tests were conducted since a preliminary analysis of the data indicated that, because of the low pressure capabilities of the blower employed, even the maximum obtainable C_Q was much too low.

Corrections.- The data have been corrected for air-stream misalinement, blocking effects, and jet-boundary effects. The jet-boundary corrections follow the method outlined in reference 4 for semispan wings. The data obtained during the boundary-layer-control tests have been adjusted for the tare effects of the ducting installation and the blowing

test results were also corrected for the thrust effect due to ejecting the air from the wing. The drag data obtained during the suction and blowing tests have not been corrected for the drag equivalent of the blower power requirements since, for these tests, the requirements are considered unrealistic because of the high duct losses which resulted in much greater values of C_p than would be expected in an operational installation. The rolling-moment correction for the effects of the reflection plane, as discussed in reference 2, was obtained from unpublished results based on the methods of references 5 and 6.

RESULTS AND DISCUSSION

The results of this investigation are presented in the following manner. The effects of deflecting the trailing-edge flaps are shown in figure 4, and figure 5 presents the effect of blowing air over the deflected flap, $\delta_f = 60^\circ$. Figure 6 offers a comparison of the characteristics provided by the slat and leading-edge flap with the trailing-edge flap neutral and deflected 45°. The results of the boundary-layer control suction tests are given in figure 7. Figures 8, 9, and 10 present the effects of various fence arrangements. Figure 11 gives, as a function of lift coefficient, the lift-drag ratios of some of the more significant wing configurations. The effectiveness of the flap-type aileron, both alone and in conjunction with stall-control devices, is illustrated in figures 12 and 13.

Lift Characteristics

The data for the basic wing (fig. 4) show an inflection in the wing lift curve at a C_L of about 0.5 due to the effect of the leading-edge separation vortex. A maximum lift coefficient of about 1.00 is obtained for the basic wing. (For a detailed discussion of the longitudinal force and flow characteristics of the basic wing, see ref. 1.)

Deflecting the plain trailing-edge flap, without blowing, produced an increment in $C_{L_{max}}$ which increased from 0.05 for a flap-deflection angle of 30° to 0.08 for flap-deflection angles of 45° and 60°, figure 4(a). The increments in lift coefficient at $\alpha = 0^\circ$ effected by deflecting the trailing-edge flap 30°, 45°, and 60° were 0.26, 0.32, and 0.36, respectively. The wing lift curves, flap deflected, are generally similar to that obtained for the basic wing, though the inflection due to the separation vortex occurs at a higher lift coefficient, about 0.6 for the two largest flap deflections, and the angle of attack for $C_{L_{max}}$ is about 3° to 4° lower.

[redacted]

Flow surveys, employing wool-strand tufts attached directly to the wing surface, indicated that for the subject wing, even at zero angle of attack, the flow over the upper surface of the deflected trailing-edge flap ($\delta_f = 45^\circ$) was stalled. In an attempt to improve this stalled condition, high-energy air was blown over the deflected trailing-edge flap, approximately tangent to the upper surface of the flap, through a spanwise slot located at the wing-flap gap as shown in figure 3. In addition, as suggested by reference 7, the upper surface of the forward portion of the flap was modified to provide a thicker, more bulbous shape, which permitted the ejected air to impinge more directly on the flap surface (fig. 3). The results of reference 7 indicate that significant increases in lift may be obtained by means of the blowing technique. In order to increase the available C_Q for the blowing tests reported in this present paper, the free-stream velocity was reduced; however, because of the scale effects shown in reference 1 for this wing, a Reynolds number of 4.4×10^6, was the lowest test value employed. At this Reynolds number a C_Q of 0.007 and a velocity ratio (ratio of the blowing air exiting velocity to the free-stream velocity) of about 1.3 were obtained, which, based on the results of other studies, still appear to be far too small to produce any "near-optimum" results.

The result of this preliminary blowing test, then, was a $C_{L_{max}}$ of 1.19 (fig. 5(a)) which was an increase of 0.11 over that obtained with the plain trailing-edge flap deflected ($\delta_f = 60^\circ$) at a Reynolds number of 6.1×10^6. Of this increment 0.08 is attributed to the blowing and 0.03 to the flap-contour modification (compare figs. 4 and 5). At zero angle of attack, the modification to the flap contour and the blowing were quite effective and resulted in C_L increases of about 0.10 and 0.05, respectively, above that obtained with the plain trailing-edge flap. No change in lift-curve slope occurred as a result of the boundary-layer control by blowing.

The results of the tests of boundary-layer control by suction are given in figure 7, but are inconclusive due to the limited C_Q obtained. Reference 3, however, shows that for a similar slot arrangement on a similar wing plan form, a $\Delta C_{L_{max}}$ of 0.15 at a C_Q of 0.028 was obtained on the unflapped wing. It should be noted, however, that the airfoil of reference 3 had a streamwise thickness of about 0.09c which would be expected to give a somewhat higher $\Delta C_{L_{max}}$ than the 0.06c section employed for these tests.

The wing lift characteristics obtained with the outboard $0.50\frac{b}{2}$ leading-edge flap and the outboard $0.50\frac{b}{2}$ slat (fig. 6(a)) are closely comparable. The effects of the two leading-edge devices are also similar with the trailing-edge flap deflected.

[redacted]

The maximum increases in $C_{L_{max}}$ realized for the various fence configurations investigated were of the order of 0.03 (figs. 8, 9, and 10).

Pitching-Moment Characteristics

The $0.50\frac{b}{2}$ slat and leading-edge flap produced very similar pitching-moment characteristics (fig. 6(b)). Although the unstable break in the pitching-moment characteristics occurs at a lower value of C_L with either device than with the basic wing (fig. 4(b)), this break is much less severe.

The effects on the longitudinal characteristics of these two devices, which are set at the same deflection, are nearly identical despite the rather large physical differences between them. It appears that the 50 percent greater chord length of the slat, its airfoil-shape contour, and the wing-slat gap contribute little, if any, to its effectiveness in pitch when applied to the subject wing of 49° leading-edge sweepback. As discussed in the subsequent section entitled "Aileron Characteristics," however, the slat was more effective than the leading-edge flap in improving the rolling characteristics of the flap-type aileron in the high angle-of-attack range.

Deflection of the plain trailing-edge flap alone (fig. 4) extends the lift coefficient at which the sharp unstable break in the pitching moment occurs from about 0.6 to about 0.75.

The deflection of the leading-edge flap or slat in conjunction with the trailing-edge flap (fig. 6) produces, in the moderate lift range, an effect similar to but not quite as stabilizing as that obtained when these devices are employed on the basic wing. However, the wing remains completely unstable above a lift coefficient of about 0.75.

The effect of the limited degree of boundary-layer control by suction on stability (fig. 7(b)) indicates that the unstable pitching-moment break is delayed about 0.15 in C_L when the suction is employed in conjunction with the $0.50\frac{b}{2}$ leading-edge flap.

A fence configuration composed of parts 3 and 4 (fig. 3), and hereafter referred to as the main fence arrangement, was tested at three spanwise locations, $0.45\frac{b}{2}$, $0.50\frac{b}{2}$, and $0.55\frac{b}{2}$, on the wing with the outboard leading-edge slat installed (fig. 8). The addition of the main fence further reduces the severity of the unstable break in the pitching

moments and delays its occurrence from a C_L of 0.50 to about 0.65. However, there seems to be little effect of varying the spanwise location of the fence for the limited range of locations tested.

Also tested on the wing with the outboard leading-edge slat installed were several different lengths and chordwise locations of a fence at the $0.50\frac{b}{2}$ station, and these results are presented in figure 9. A study of figure 9(b) reveals that the pitching characteristics obtained with the main fence are not significantly altered by the addition of the forward-located sections, parts 1 and 2. However, a comparison of the data in figures 8 and 9 indicates that installing a small end plate on the inboard end of the slat (part 1 of the fence, fig. 3) appears to improve slightly the aerodynamic characteristics, in the high-lift range below stall, of the wing with the slat extended.

Two fence configurations were tested at the $0.50\frac{b}{2}$ station on the wing with the outboard slat and trailing-edge flap installed, and the results of these tests are shown in figure 10. In general, the effects of the fence are similar to those previously described for the configuration with the slat deflected alone.

In evaluation of these stall-control devices in terms of over-all airplane stability, consideration should be given to the probable effect of these devices on the effectiveness of the horizontal tail in addition to the wing-alone stability changes indicated herein (see, for example, refs. 8 and 9).

Drag Characteristics

For the test configuration of blowing air over the deflected trailing-edge flap, a drag reduction was realized even for the low C_Q employed (fig. 5(c)). The probable cause of this drag reduction is the energy imparted to the stalled flow over the 60° deflected flap by the exiting blowing air. It should be noted, however, that as previously mentioned in the section entitled "Tests and Corrections," the drag results discussed herein do not include the effects of blower power drag.

In the case of the suction slot, however, the low available C_Q was probably too small to prevent flow separation at the lips of the suction slot and a drag penalty was incurred (fig. 7(c)).

The highest value of L/D obtained in this investigation (fig. 11) was approximately 17 and was reached with the basic wing at a C_L of about 0.28. In the high lift range, the best L/D ratio was obtained

with the trailing-edge flap deflected 45° in combination with either the leading-edge flap or slat. This configuration produced a maximum L/D of about 7.5 at a C_L of about 0.68.

Aileron Characteristics

The variation with angle of attack of the rolling-moment coefficient due to deflecting one aileron (left wing panel) is shown in figure 12. For the basic wing configuration, below about $\alpha = 12°$, the data appear linear in that proportional increases in rolling-moment coefficient are realized for increases in span and deflection. In the higher α range, above about $\alpha = 12°$, there is a marked decrease in effectiveness of the aileron. The estimated C_l values, calculated by the method of reference 10, are somewhat optimistic in the high α range for the $0.15\frac{b}{2}$ - span aileron and over the entire α range for the $0.39\frac{b}{2}$ - span aileron.

Figure 13 illustrates the effect of stall-control devices, located outboard on the wing, on the rolling moments provided by the $0.39\frac{b}{2}$ - span aileron. As shown, both the slat and leading-edge flap effect large improvements in the rolling characteristics obtained with the flap-type aileron in the high α range. Above an angle of attack of about 20°, extending the slat increases the rolling moment due to aileron deflection by about 70 percent. Not only greater values of C_l but a more linear trend in the variation of C_l with α is obtained with the slat as compared to the leading-edge flap. This difference between the characteristics obtained with the leading-edge flap and the slat would appear to be paradoxical in light of their closely comparable effects on lift, drag, and pitching moment. Presumably the boundary layer toward the rear of the tip sections is thinner for the slat than for the flap, and, although the difference may not be sufficient to effect appreciably either the lift or the pitching moment, it may tend to improve the effectiveness of the deflected aileron.

CONCLUDING REMARKS

An investigation has been conducted to determine the effect of various high-lift and stall-control devices, including boundary-layer control, on the aerodynamic characteristics of a 49.1° sweptback wing having an aspect ratio of 3.78, a taper ratio of 0.586, and NACA 65A006 sections streamwise.

[redacted]

Both the leading-edge flap and slat reduced the severity of the unstable break from that obtained with the basic wing. Despite large geometric differences, the leading-edge flap and slat produce closely comparable lift, drag, and pitching-moment characteristics. When employed for improving the rolling characteristics of the aileron at the high angles of attack, however, the slat appears to be the more effective of the two stall-control devices.

At zero angle of attack, the plain trailing-edge flap produced an increment in lift coefficient of 0.36, at a flap deflection of 60°, but was relatively ineffective in increasing the maximum lift of the subject wing. Because of the limited quantity of air employed in this preliminary test, only small lift gains were realized as a result of blowing air over the deflected trailing-edge flap. In order to judge adequately the feasibility of this type of boundary-layer control as a means of increasing the maximum lift of the subject wing, additional tests with higher rates of air flow will be required.

Langley Aeronautical Laboratory
National Advisory Committee for Aeronautics
Langley Field, Va.

REFERENCES

1. Lipson, Stanley, and Barnett, U. Reed, Jr.: Force and Pressure Investigation at Large Scale of a 49° Sweptback Semispan Wing Having NACA 65A006 Sections and Equipped with Various Slat Arrangements. NACA RM L51K26, 1952.

2. Lipson, Stanley, and Barnett, U. Reed, Jr.: Comparison of Semispan and Full-Span Tests of a 47.5° Sweptback Wing with Symmetrical Circular-Arc Sections and Having Drooped-Nose Flaps, Trailing-Edge Flaps, and Ailerons. NACA RM L51H15, 1951.

3. Pasamanick, Jerome, and Proterra, Anthony J.: The Effect of Boundary-Layer Control by Suction and Several High-Lift Devices on the Longitudinal Aerodynamic Characteristics of a 47.5° Sweptback Wing-Fuselage Combination. NACA RM L8E18, 1948.

4. Sivells, James C., and Salmi, Rachel M.: Jet-Boundary Corrections for Complete and Semispan Swept Wings in Closed Circular Wind Tunnels. NACA TN 2454, 1951.

5. DeYoung, John: Theoretical Antisymmetric Span Loading for Wings of Arbitrary Plan Form at Subsonic Speeds. NACA TN 2140, 1950.

6. Swanson, Robert S., and Toll, Thomas A.: Jet-Boundary Corrections for Reflection-Plane Models in Rectangular Wind Tunnels. NACA Rep. 770, 1943. (Formerly NACA ARR 3E22.)

7. Schwier, W.: Lift Increase by Blowing Out Air, Tests on Airfoil of 12 Percent Thickness, Using Various Types of Flap. NACA TM 1148, 1947.

8. Queijo, M. J., and Wolhart, Walter D.: Wind-Tunnel Investigation of the Effects of Horizontal-Tail Position on the Low-Speed Longitudinal Stability Characteristics of an Airplane Model with a 35° Sweptback Wing Equipped with Chordwise Fences. NACA RM L51H17, 1951.

9. Salmi, Reino J.: Horizontal-Tail Effectiveness and Downwash Surveys for Two 47.7° Sweptback Wing-Fuselage Combinations with Aspect Ratios of 5.1 and 6.0 at a Reynolds Number of 6.0×10^6. NACA RM L50K06, 1951.

10. Lowry, John G., and Schneiter, Leslie E.: Estimation of Effectiveness of Flap-Type Controls on Sweptback Wings. NACA TN 1674, 1948.

[redacted]

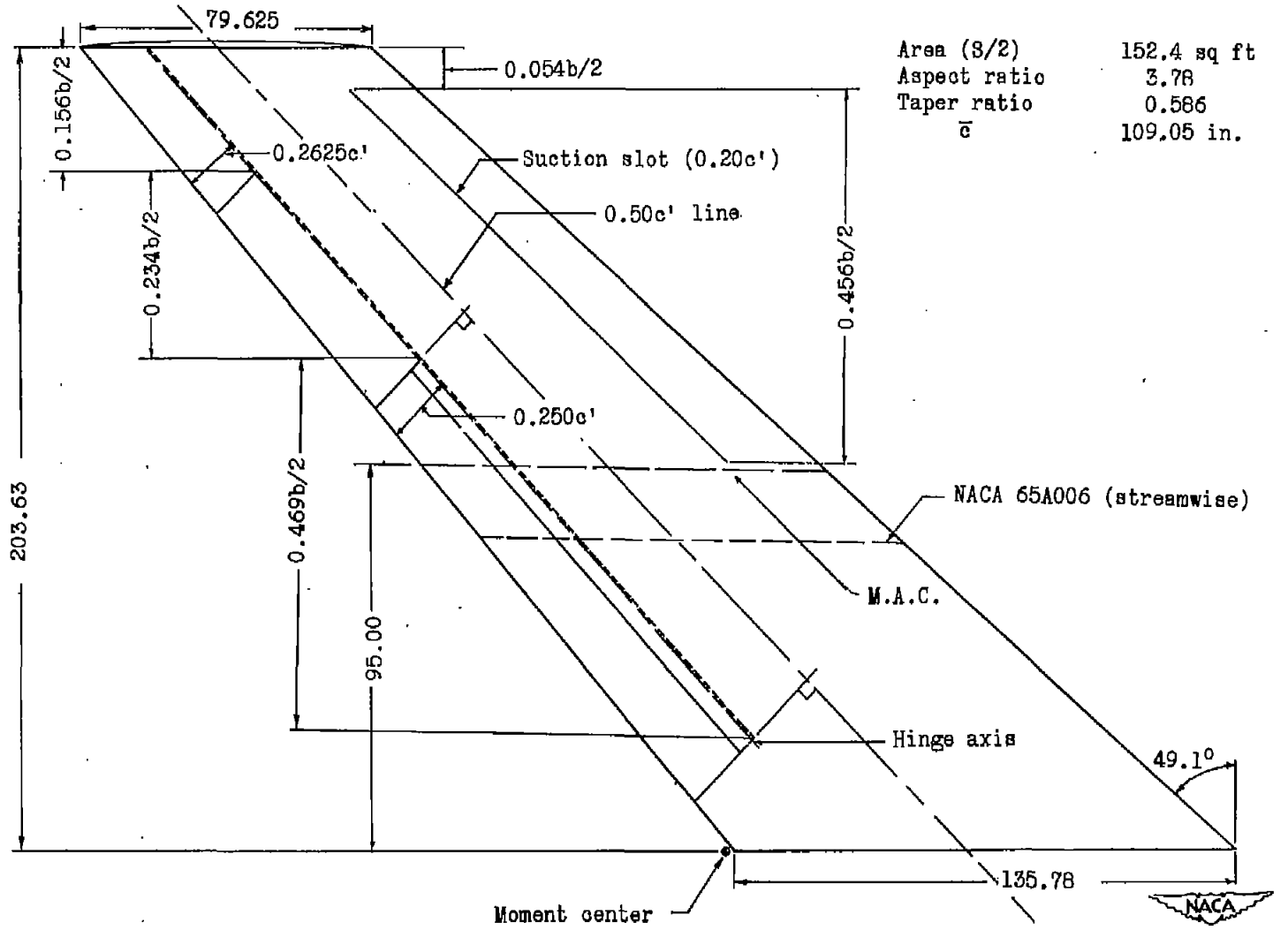

Figure 1.- Plan form of semispan 49.1° sweptback wing. All dimensions are in inches.

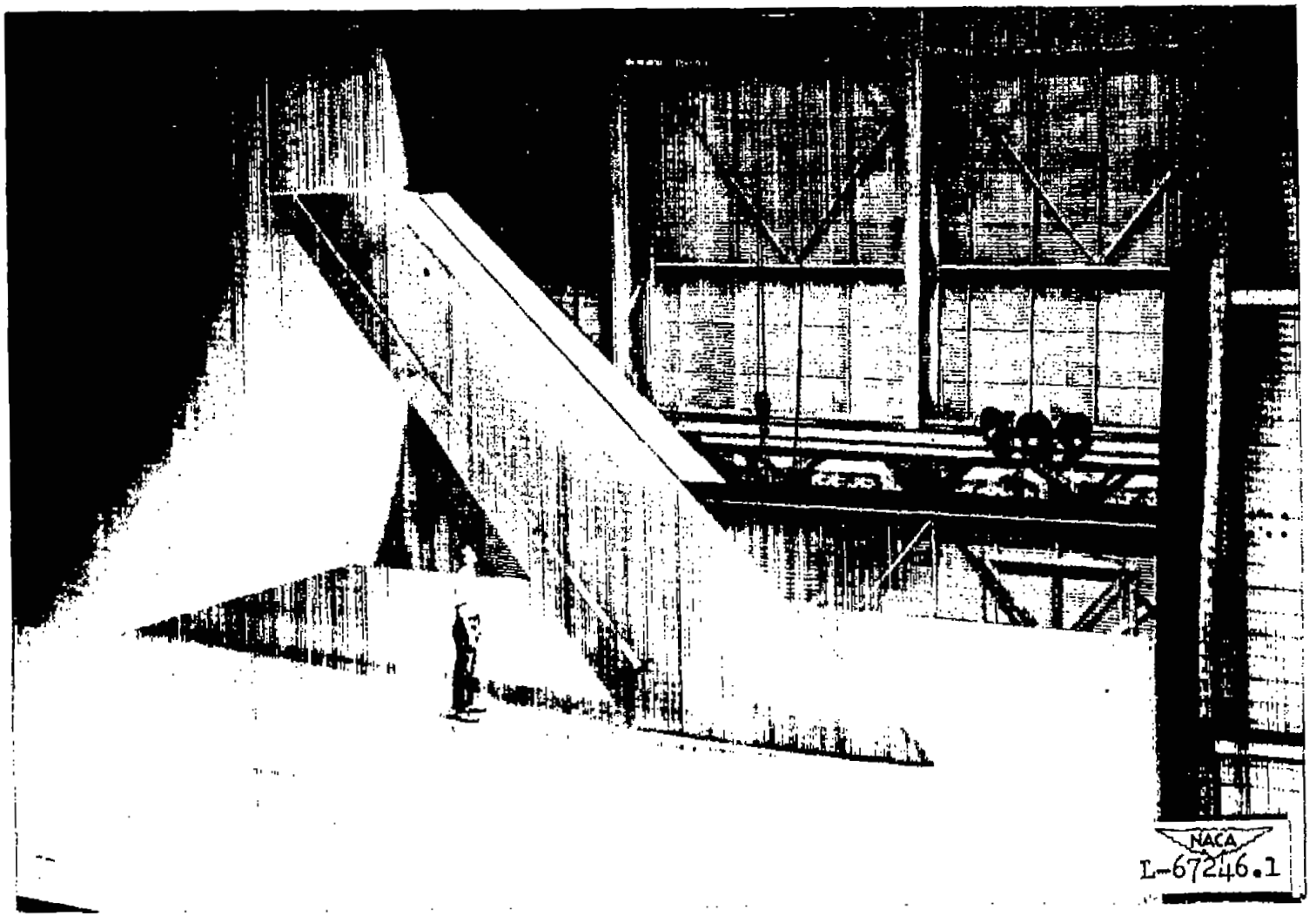

Figure 2.- The semispan 49.1° sweptback wing, with semispan slat installed, mounted in the Langley full-scale tunnel.

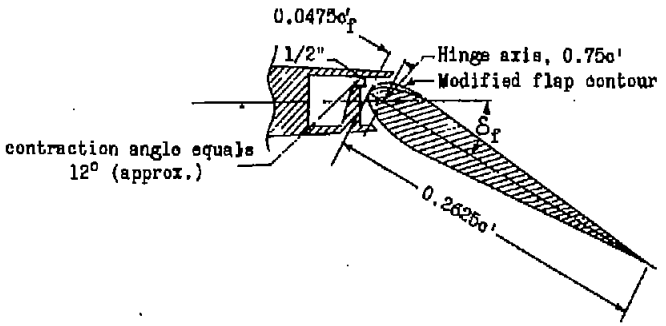

Trailing edge flap and blowing slot

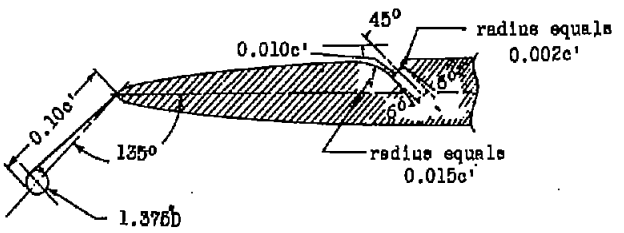

Leading-edge flap and suction slot

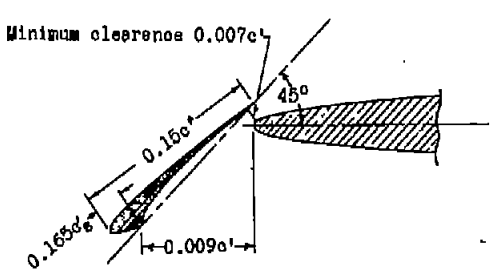

Leading-edge slat

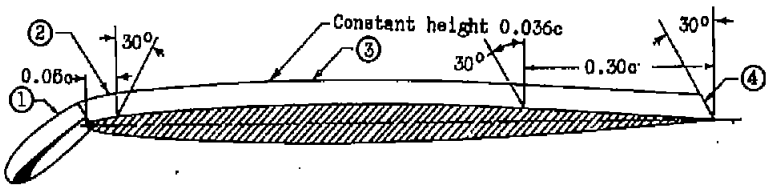

Fence

Numbers ①, ②, ③, and ④ identify four separate parts to fence.

c' is used to denote local chord length perpendicular to the midchord line.

Figure 3.- High-lift and stall-control devices tested on semispan 49.1° sweptback wing.

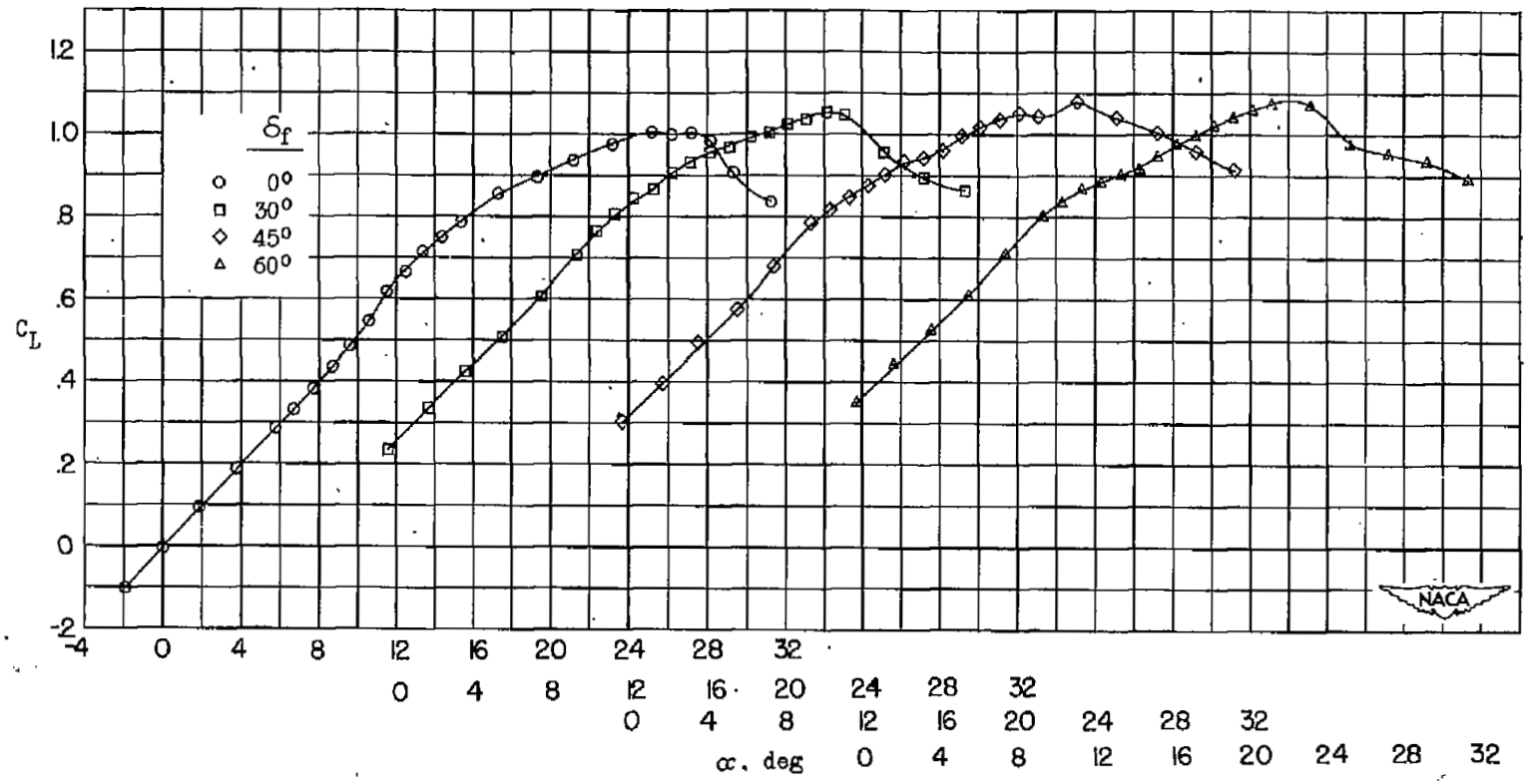

(a) Lift.

Figure 4.- The effects of trailing-edge-flap deflection on the aerodynamic characteristics of a semispan 49.1° sweptback wing.

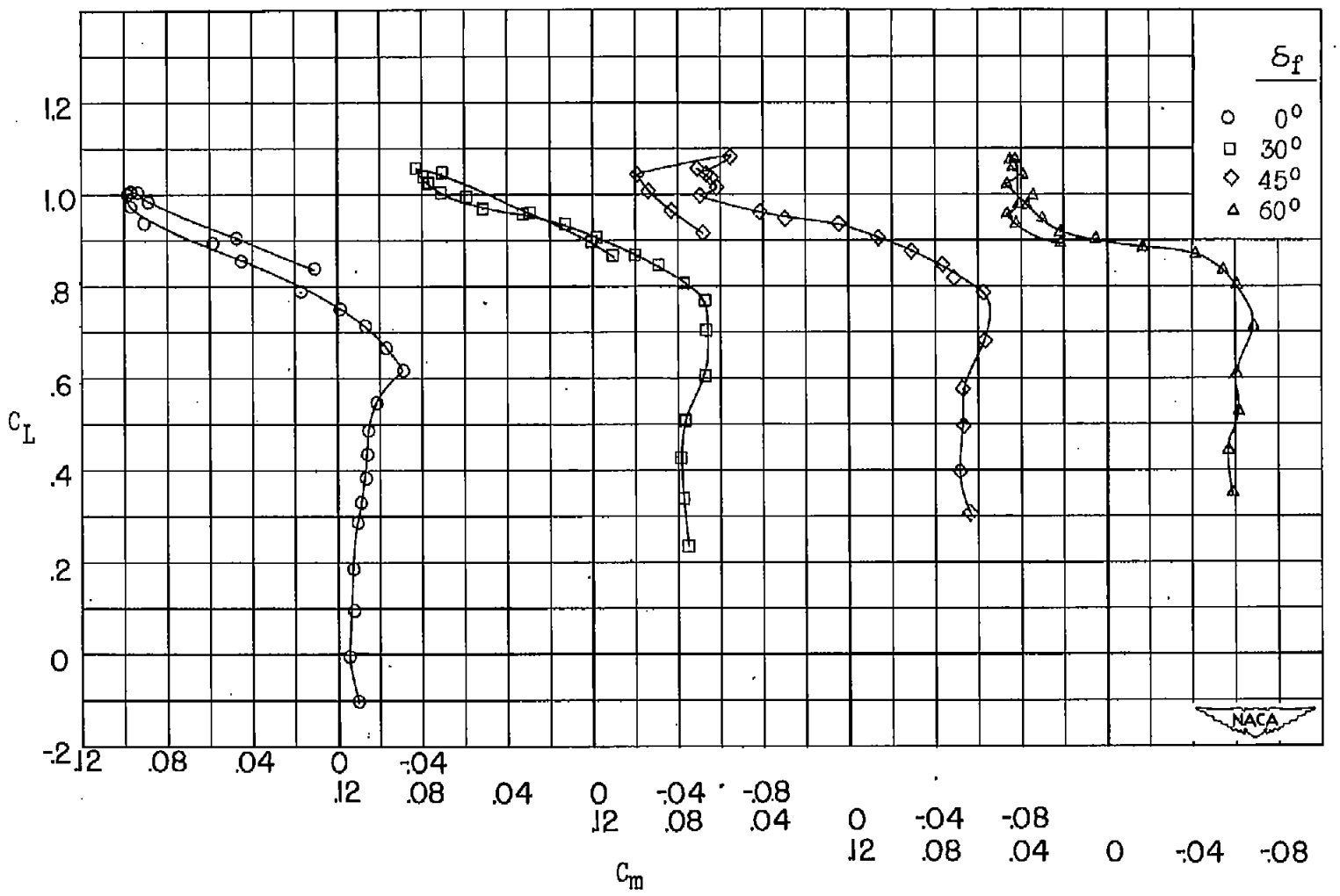

(b) Pitching moment.

Figure 4.- Continued.

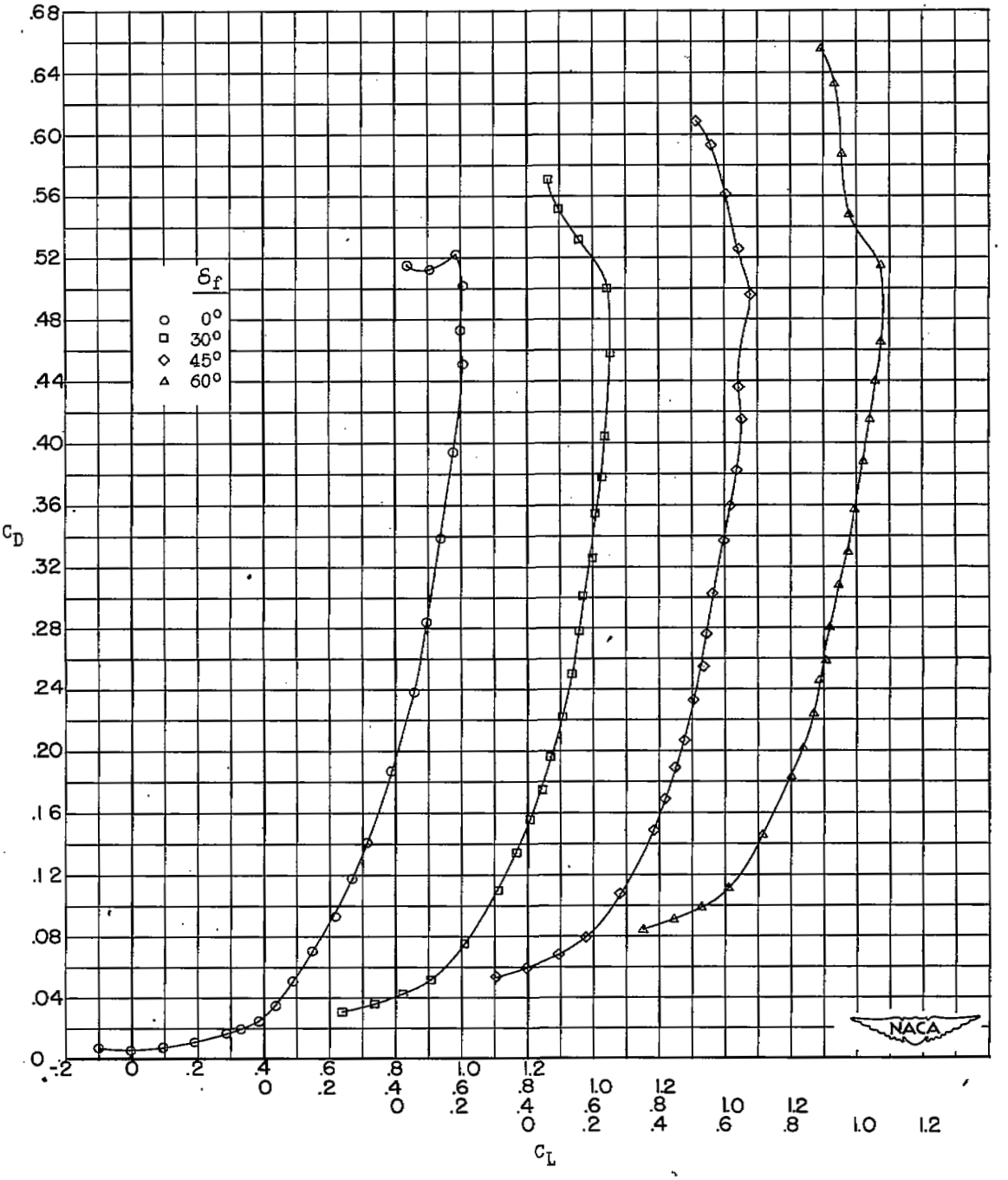

(c) Drag.

Figure 4.- Concluded.

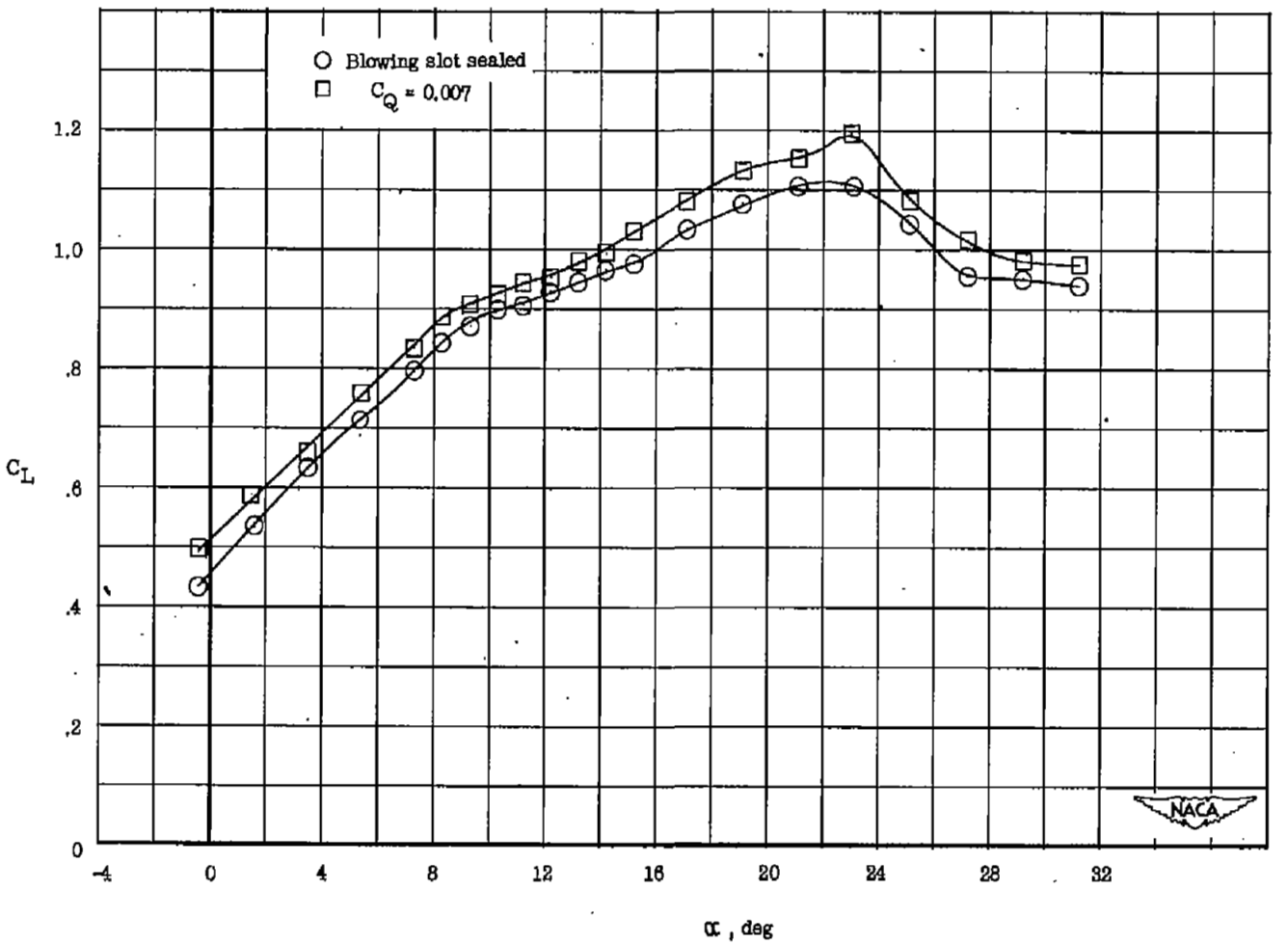

(a) Lift.

Figure 5.- The effects of blowing air over the modified trailing-edge flap on the aerodynamic characteristics of a semispan 49.1° swept-back wing. Flap deflected 60°; R = 4.4 × 10^6.

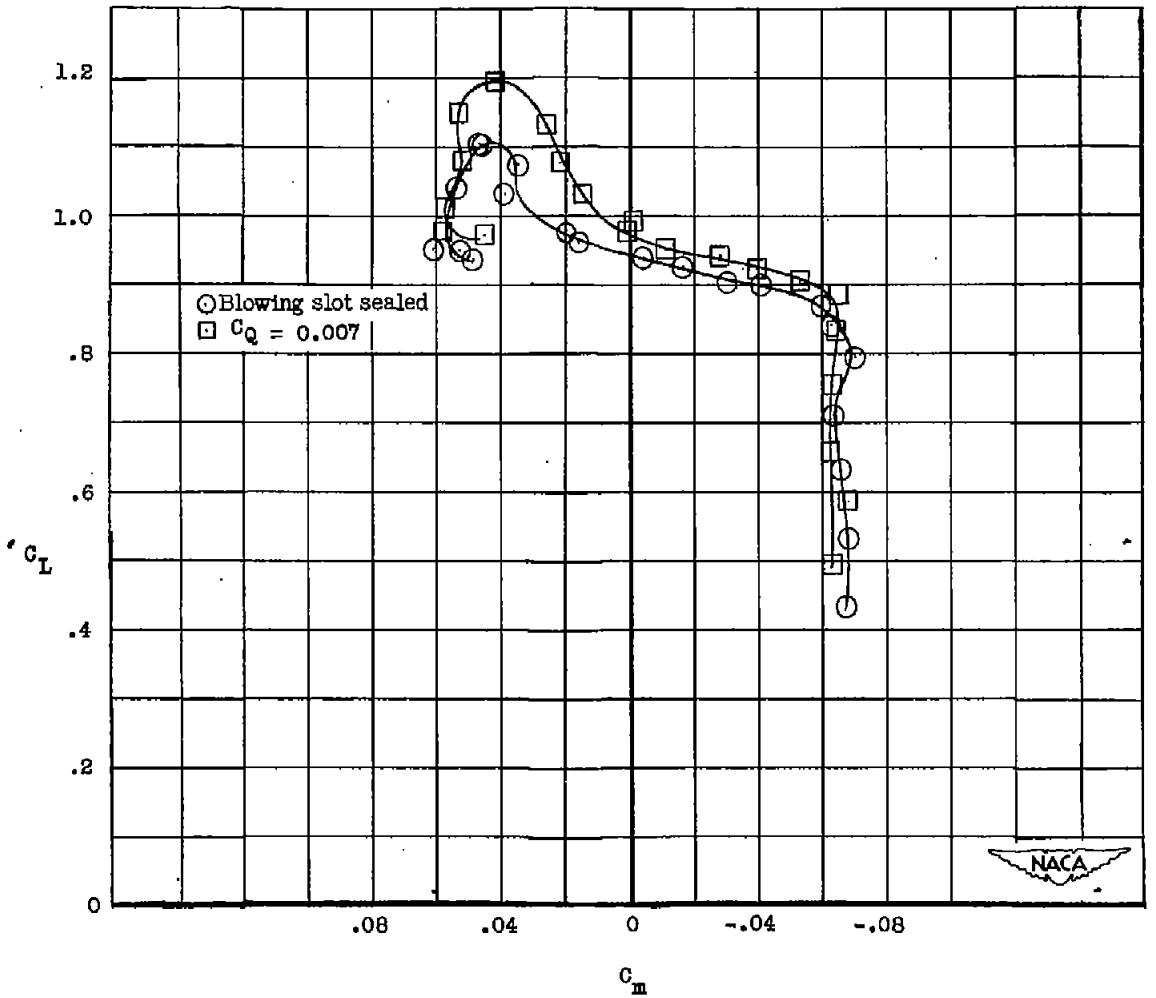

(b) Pitching moment.

Figure 5.- Continued.

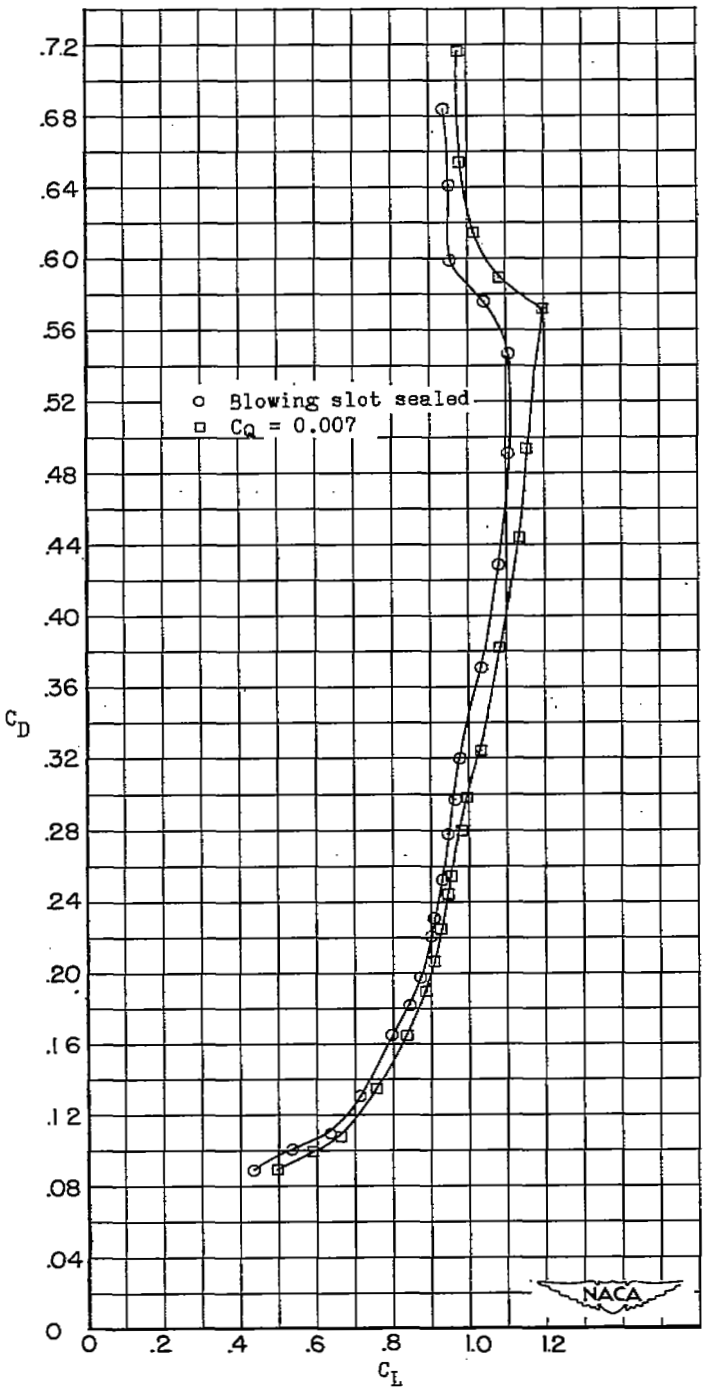

(c) Drag.

Figure 5.- Concluded.

[redacted]

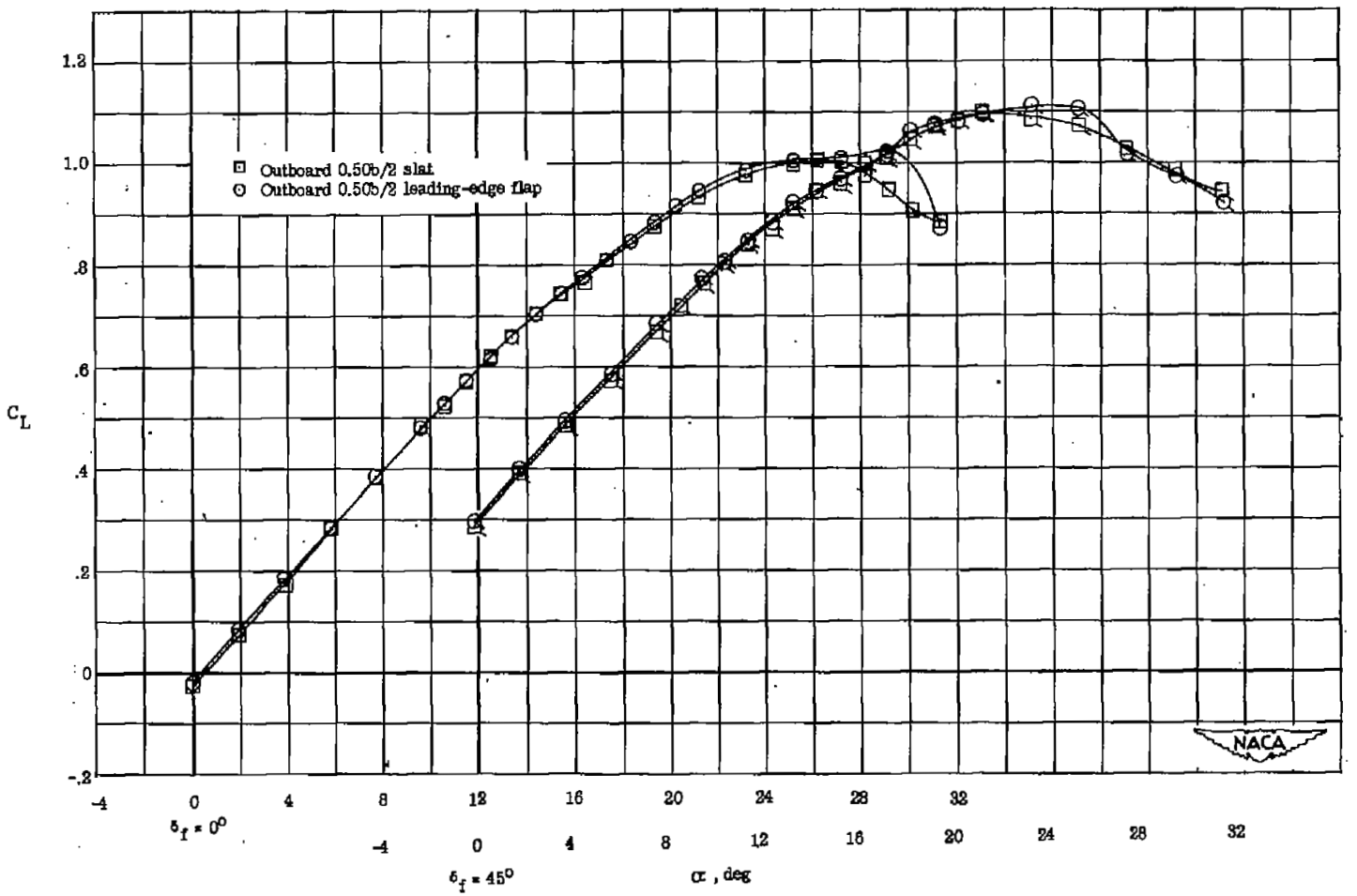

(a) Lift.

Figure 6.- The effects of leading-edge devices on the aerodynamic characteristics of a semispan 49.1° sweptback wing; trailing-edge flap neutral and deflected 45°.

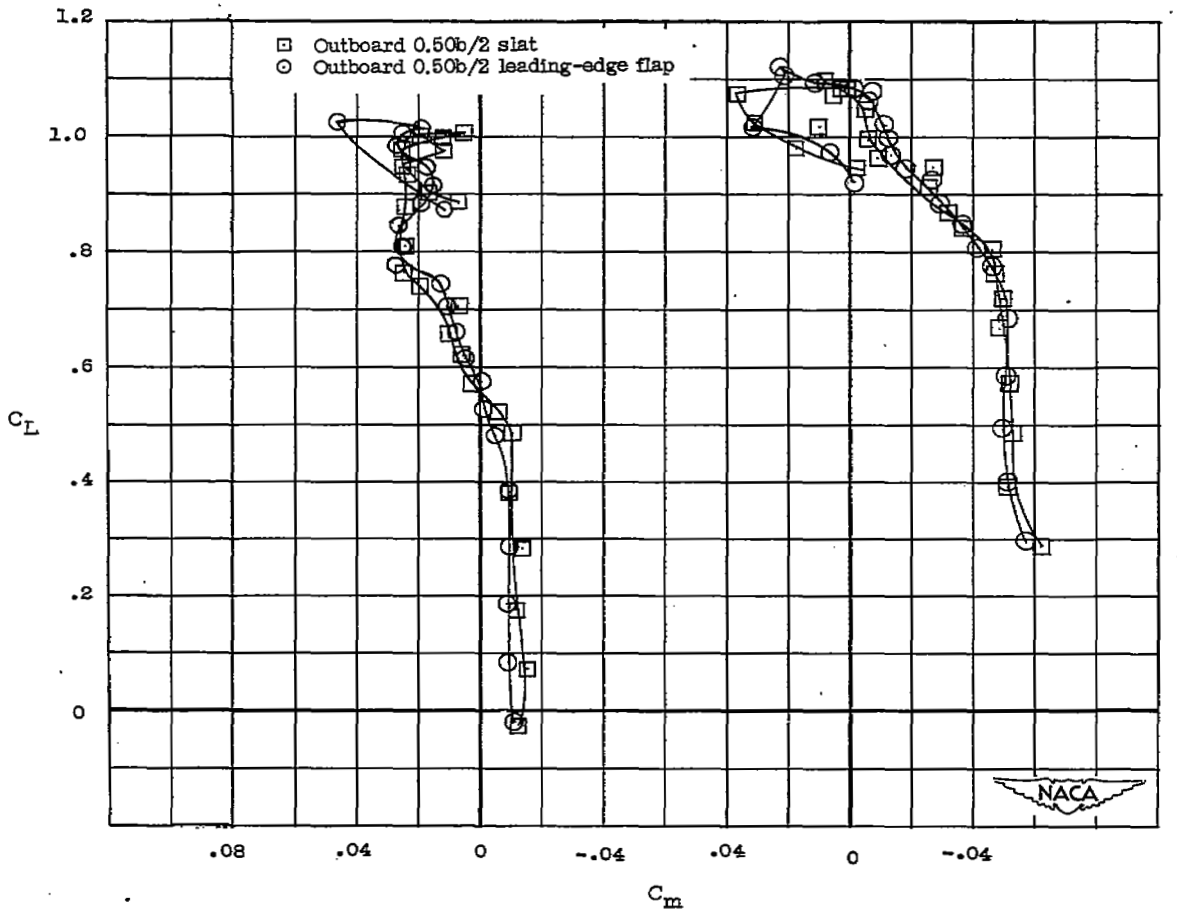

(b) Pitching moment.

Figure 6.- Continued.

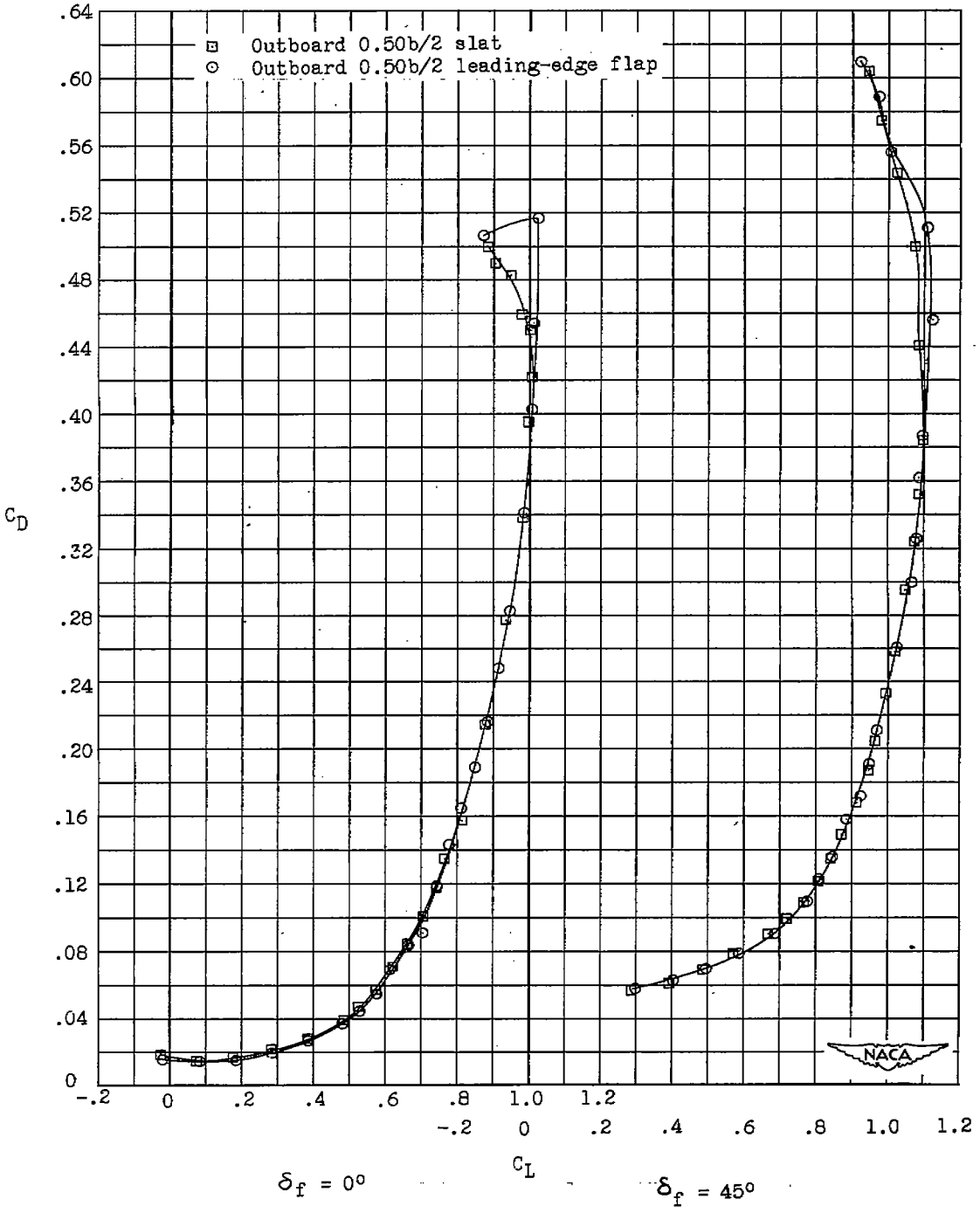

(c) Drag.

Figure 6.- Concluded.

[redacted]

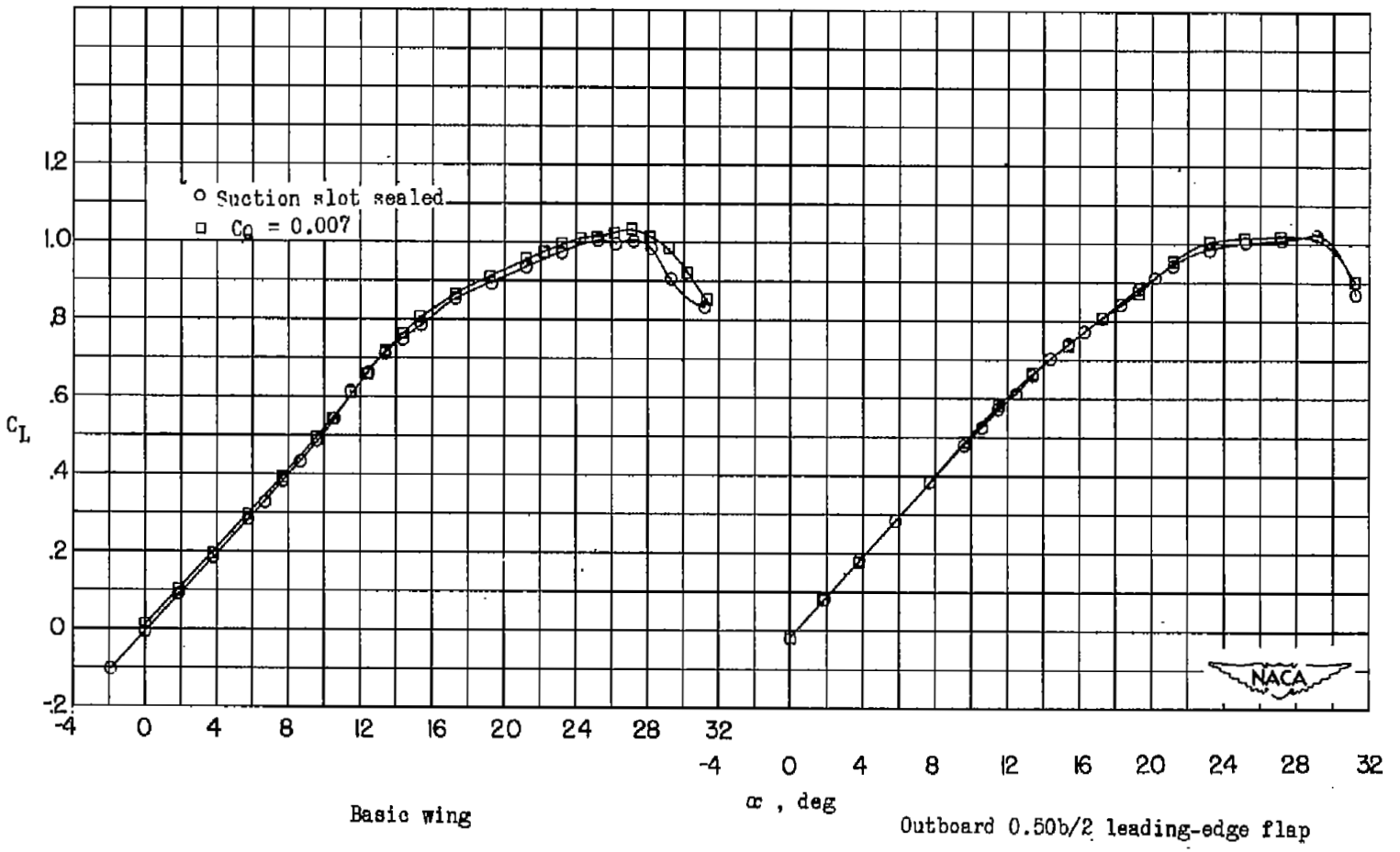

(a) Lift.

Figure 7.- The effects of boundary-layer control by suction on the aerodynamic characteristics of a semispan 49.1° sweptback wing alone and in combination with the outboard 0.50b/2 leading-edge flap. $\delta_f = 0°$.

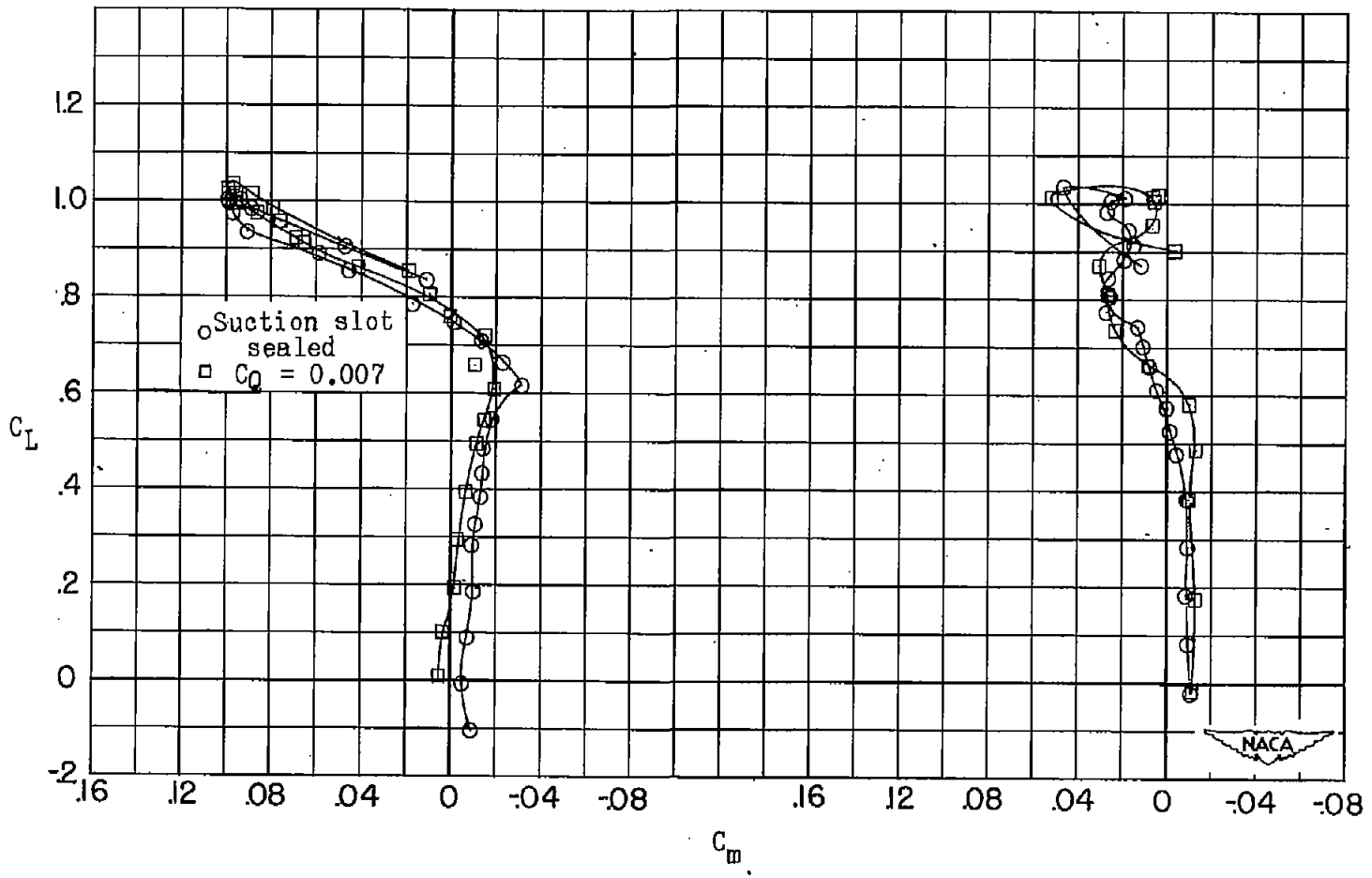

Basic wing

Outboard 0.50b/2 leading-edge flap

(b) Pitching moment.

Figure 7.- Continued.

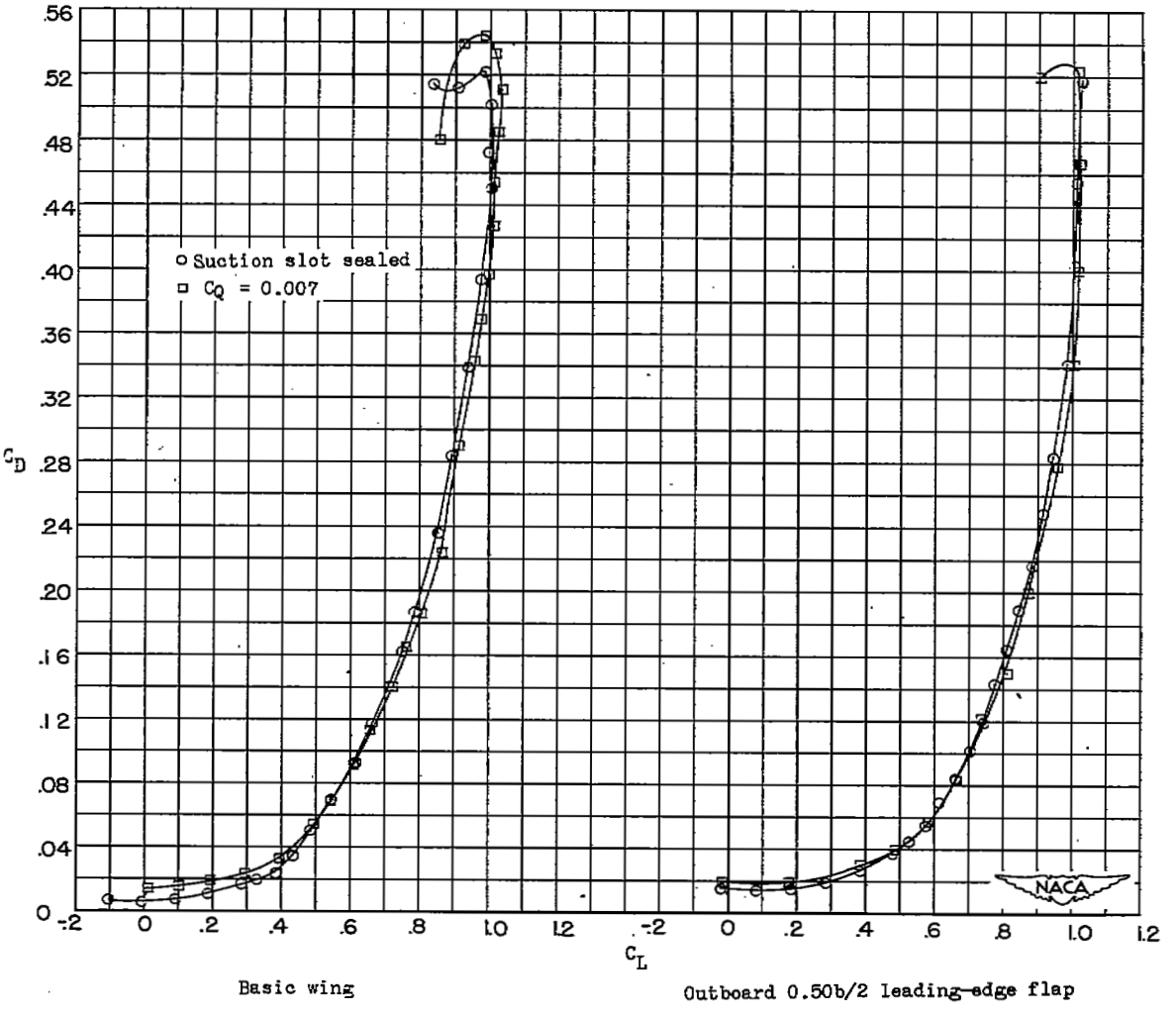

(c) Drag.

Figure 7.- Concluded.

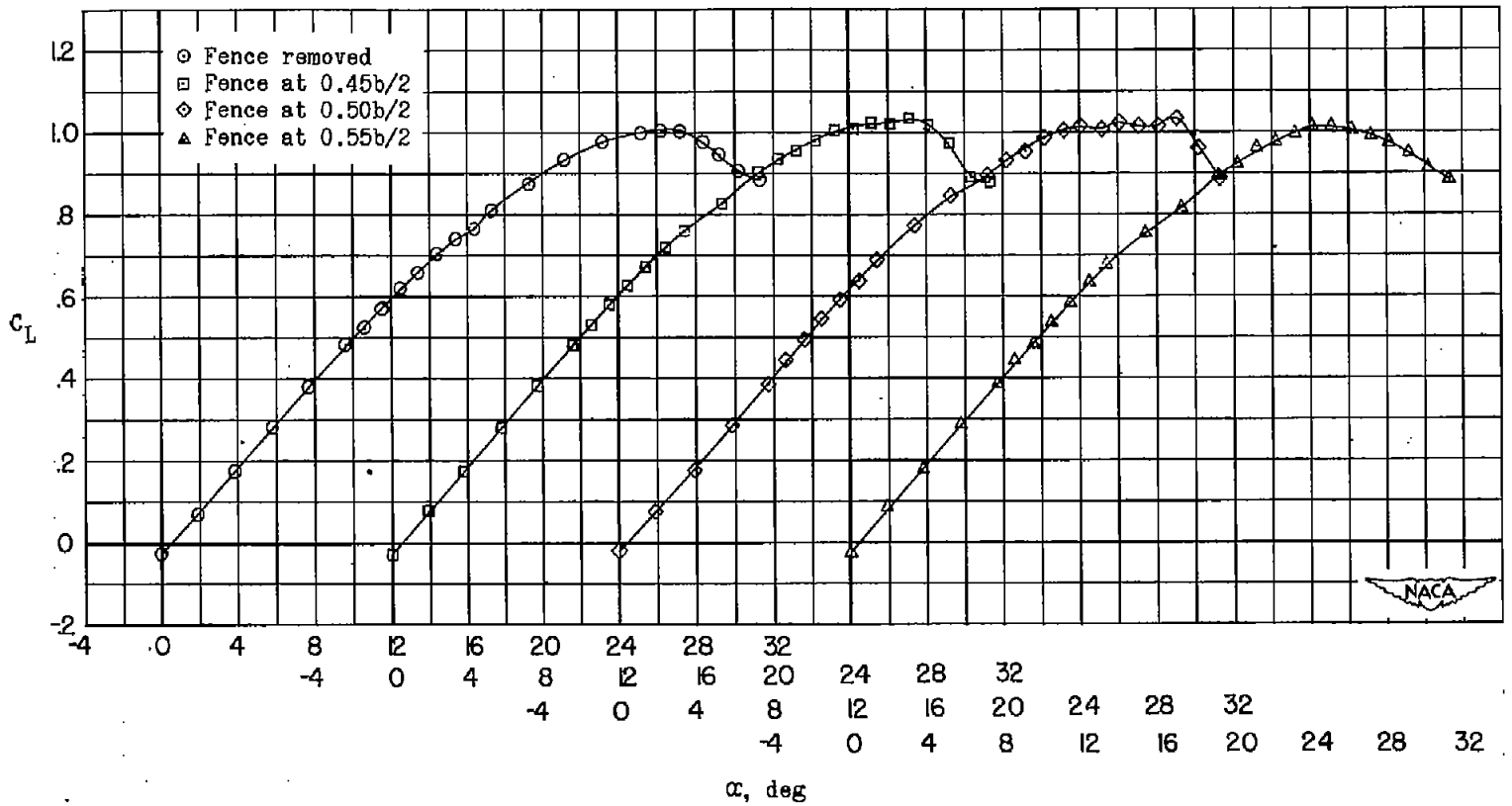

(a) Lift.

Figure 8.- The effects of spanwise location of the main fence (parts 3 and 4, fig. 3) on the aerodynamic characteristics of a semispan 49.1° sweptback wing with outboard 0.50b/2 leading-edge slat installed. $\delta_f = 0°$.

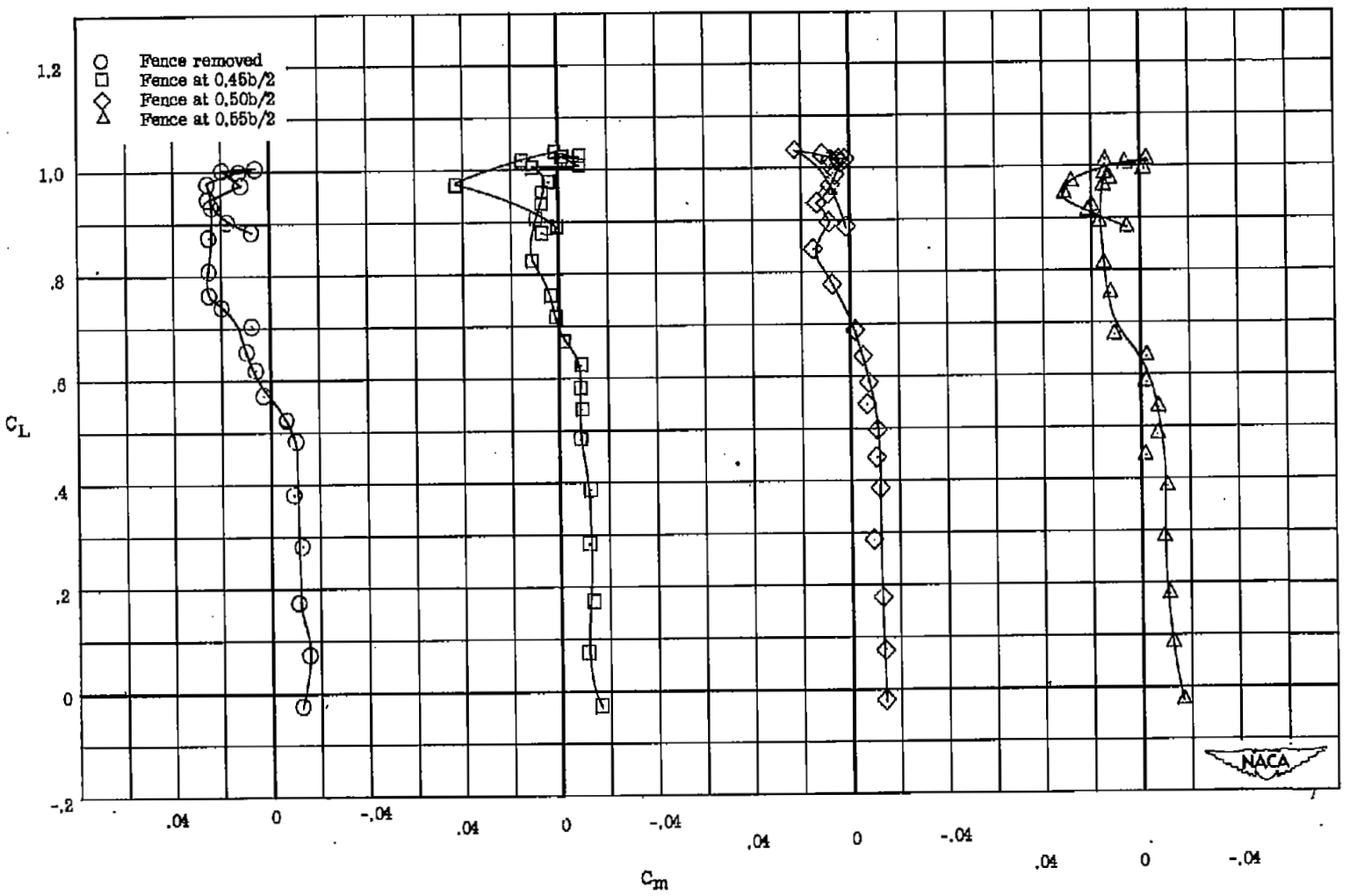

(b) Pitching moment.

Figure 8.- Continued.

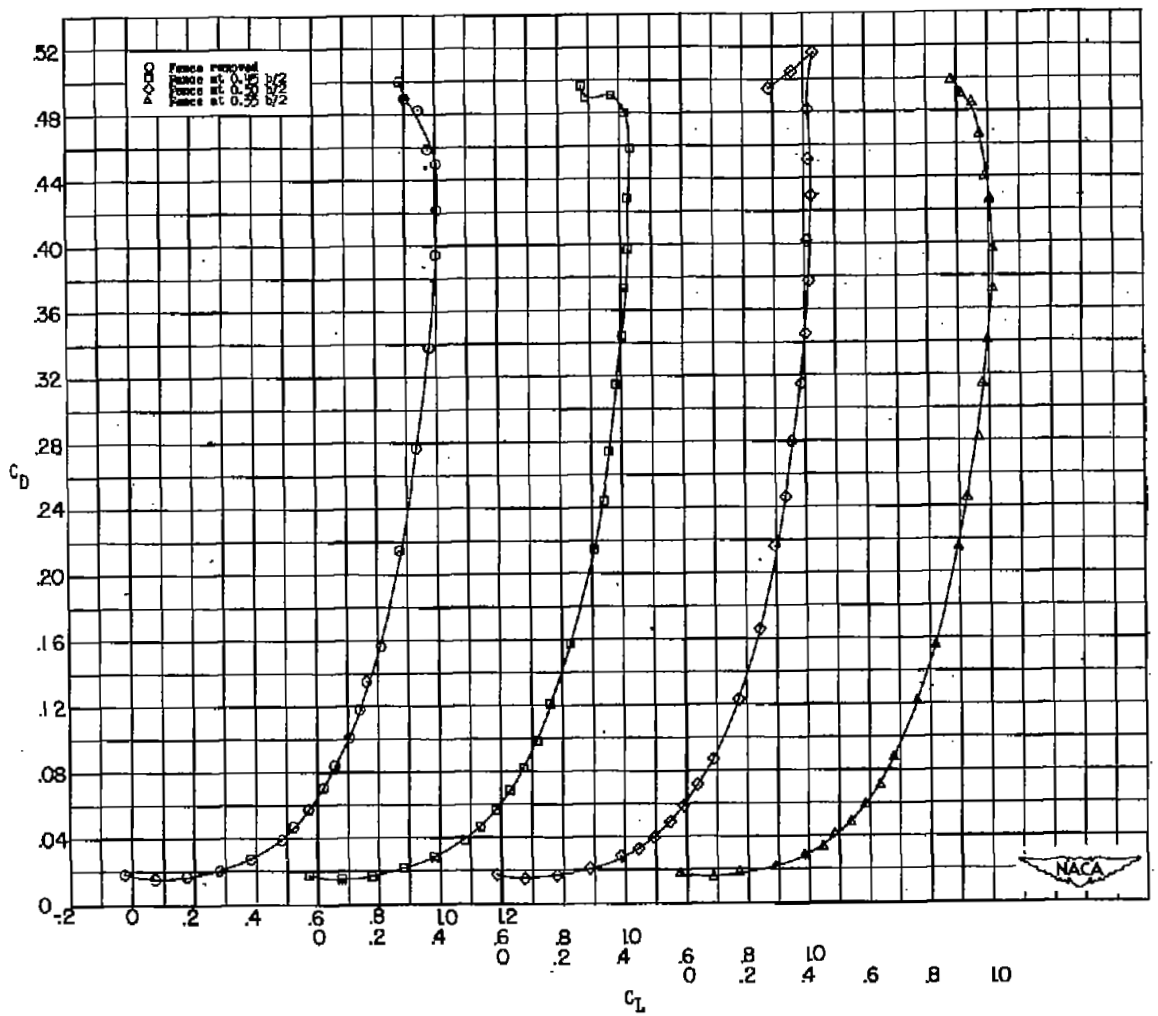

(c) Drag.

Figure 8.- Concluded.

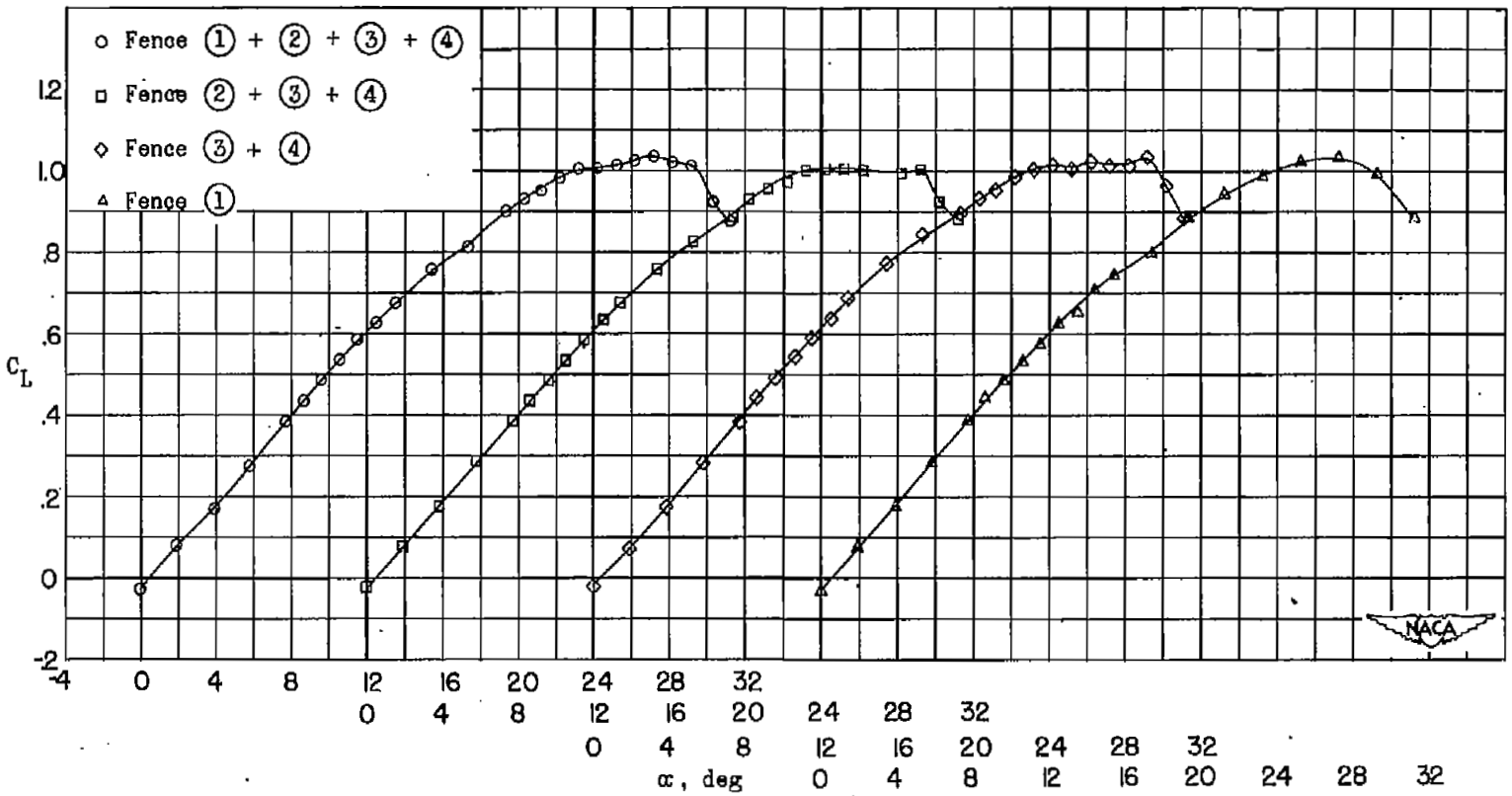

(a) Lift.

Figure 9.- The effects of several chordwise fence configurations on the aerodynamic characteristics of a semispan 49.1° sweptback wing with outboard 0.50b/2 leading-edge slat installed. Fence at 0.50b/2; $\delta_f = 0°$.

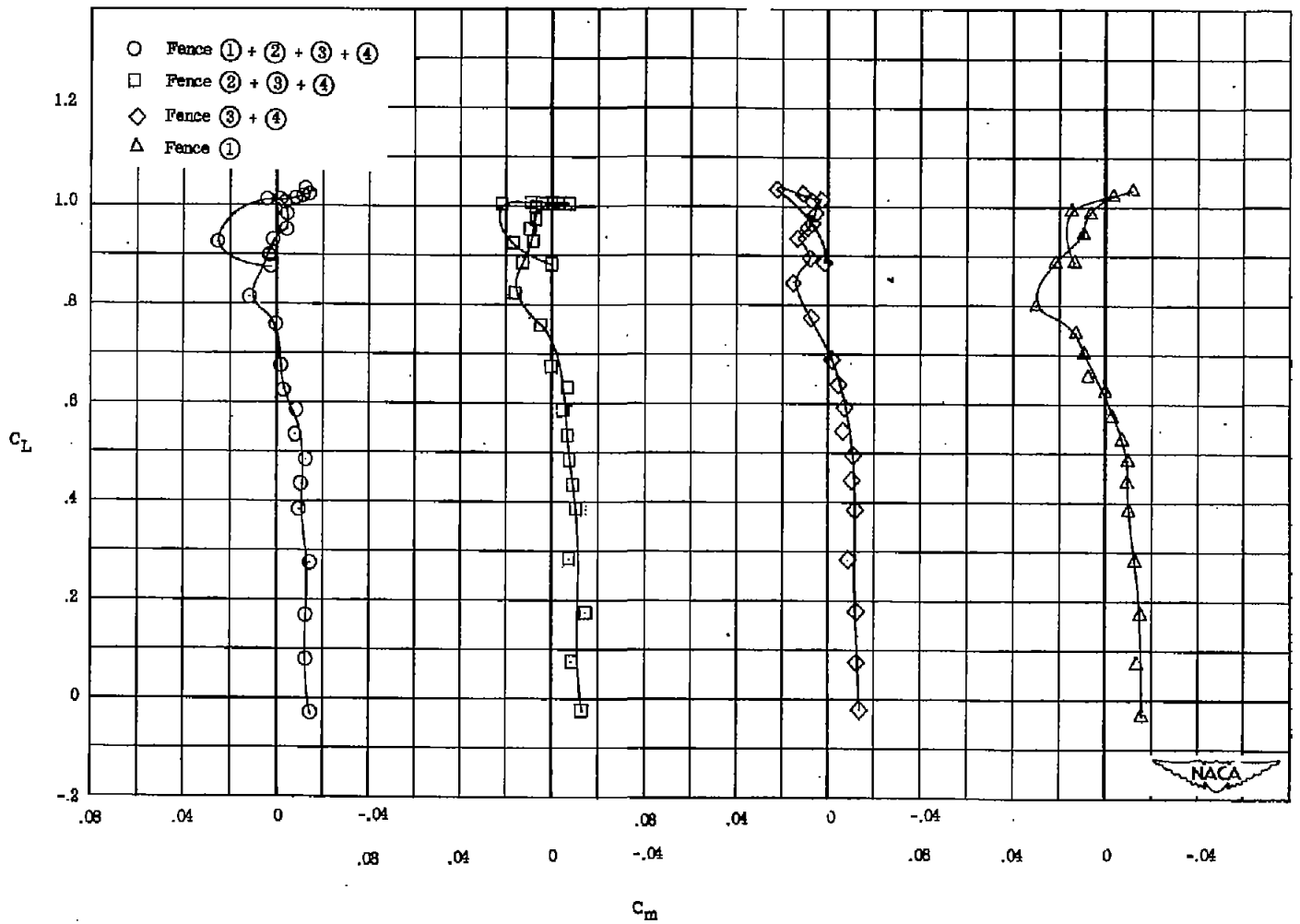

(b) Pitching moment.

Figure 9.- Continued.

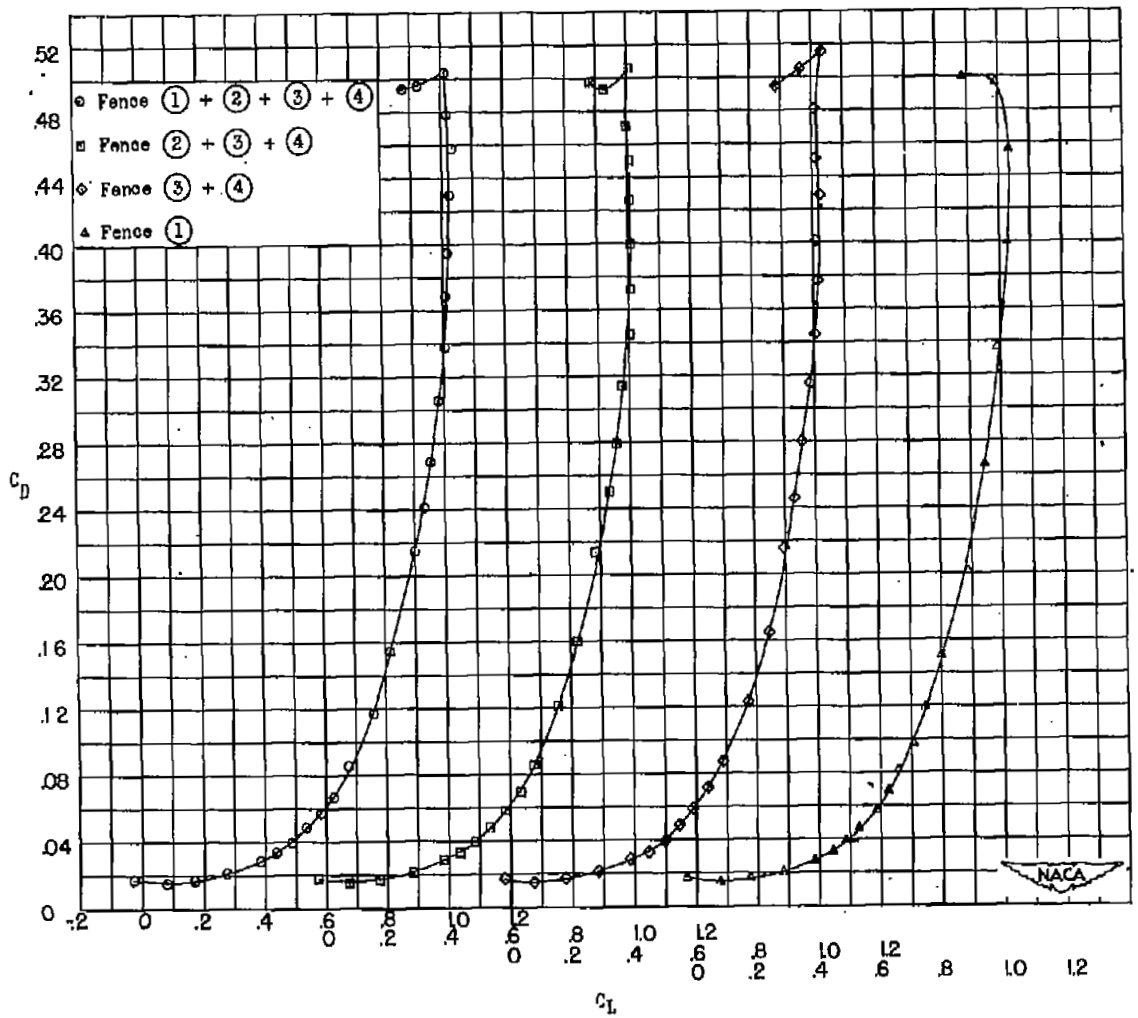

(c) Drag.

Figure 9.- Concluded.

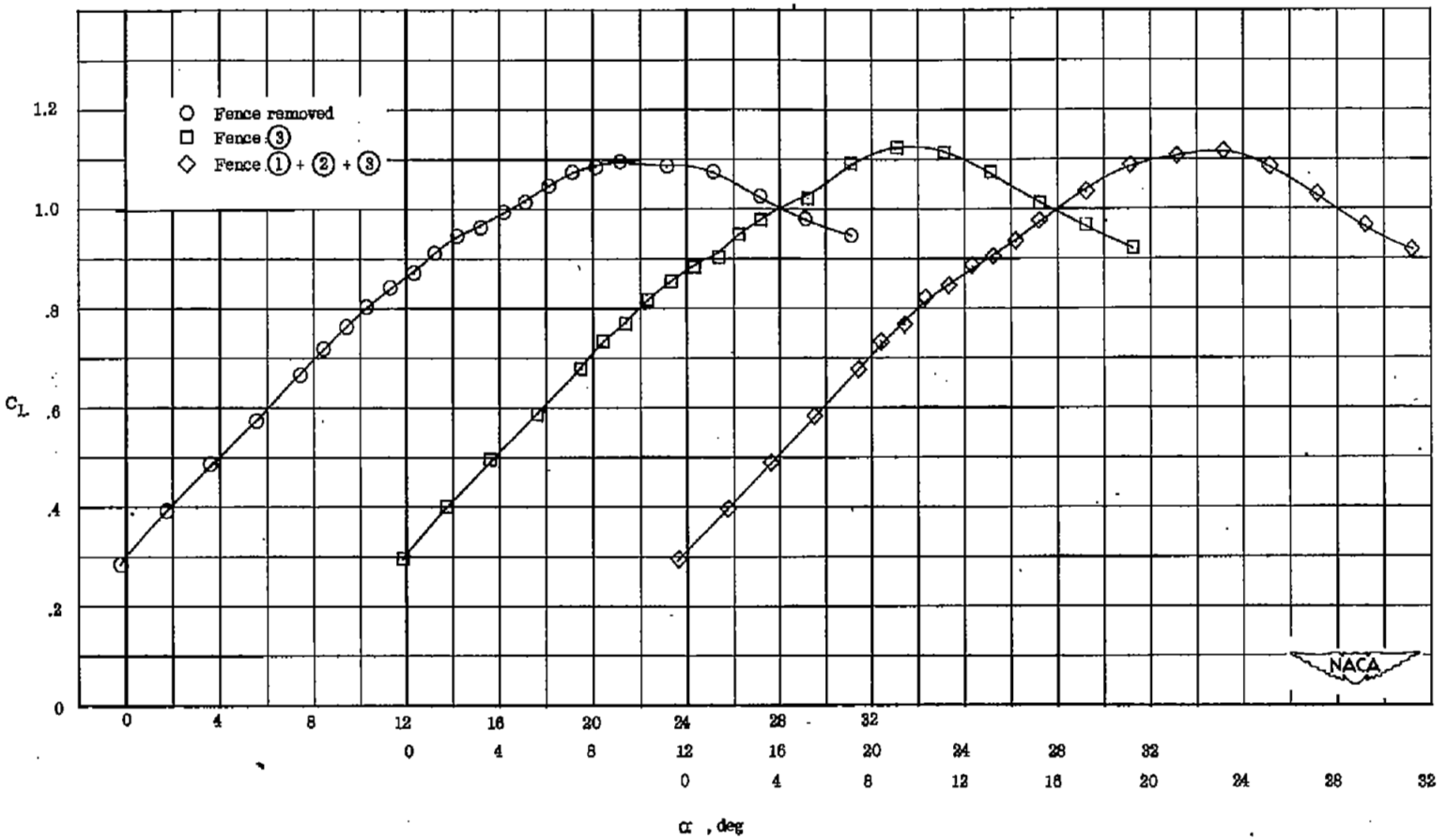

(a) Lift.

Figure 10.- The effects of a fence on the aerodynamic characteristics of a semispan 49.1° sweptback wing with outboard 0.50b/2 leading-edge slat installed and trailing-edge flap deflected. Fence at 0.50b/2; $\delta_f = 45°$.

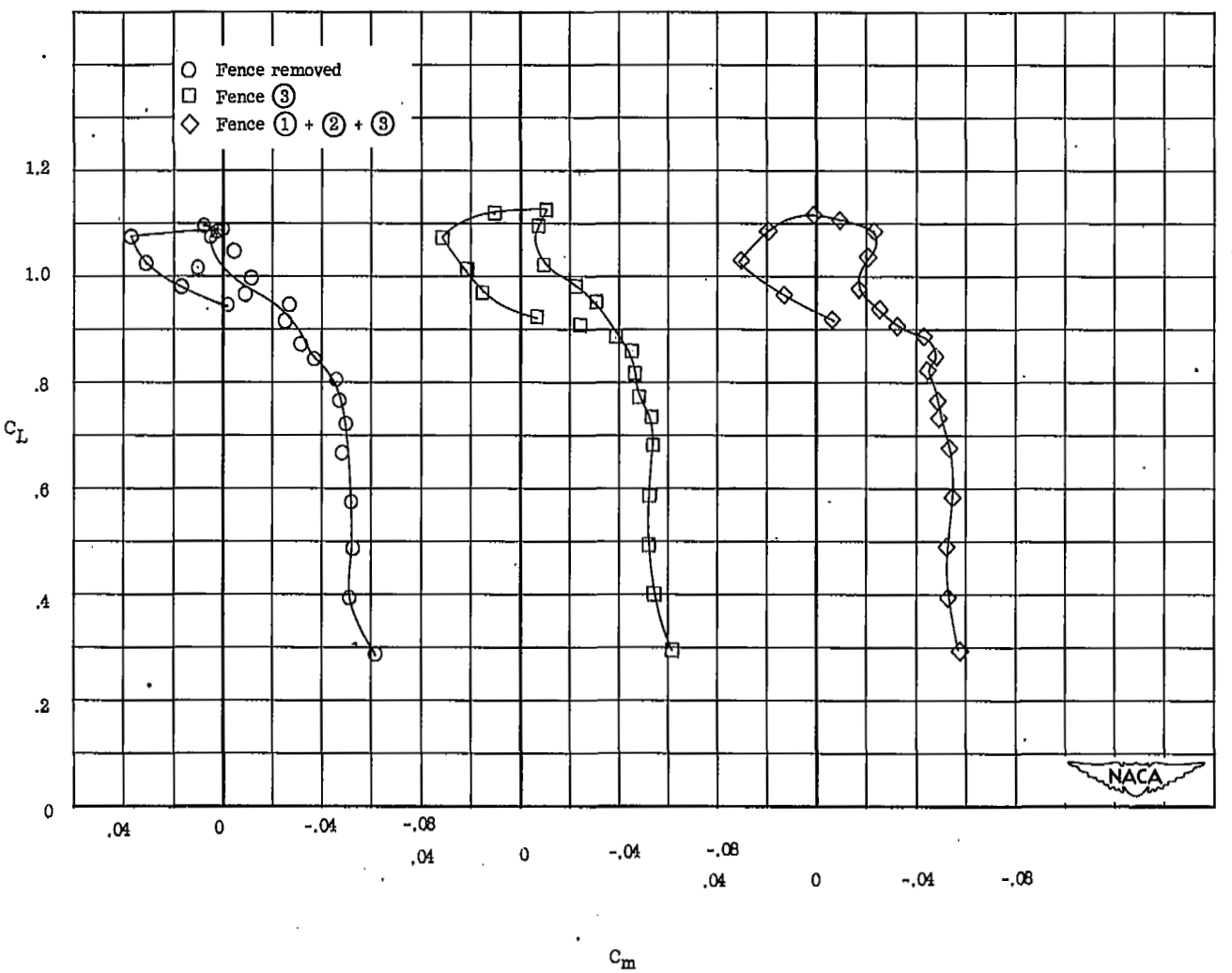

(b) Pitching moment.

Figure 10.- Continued.

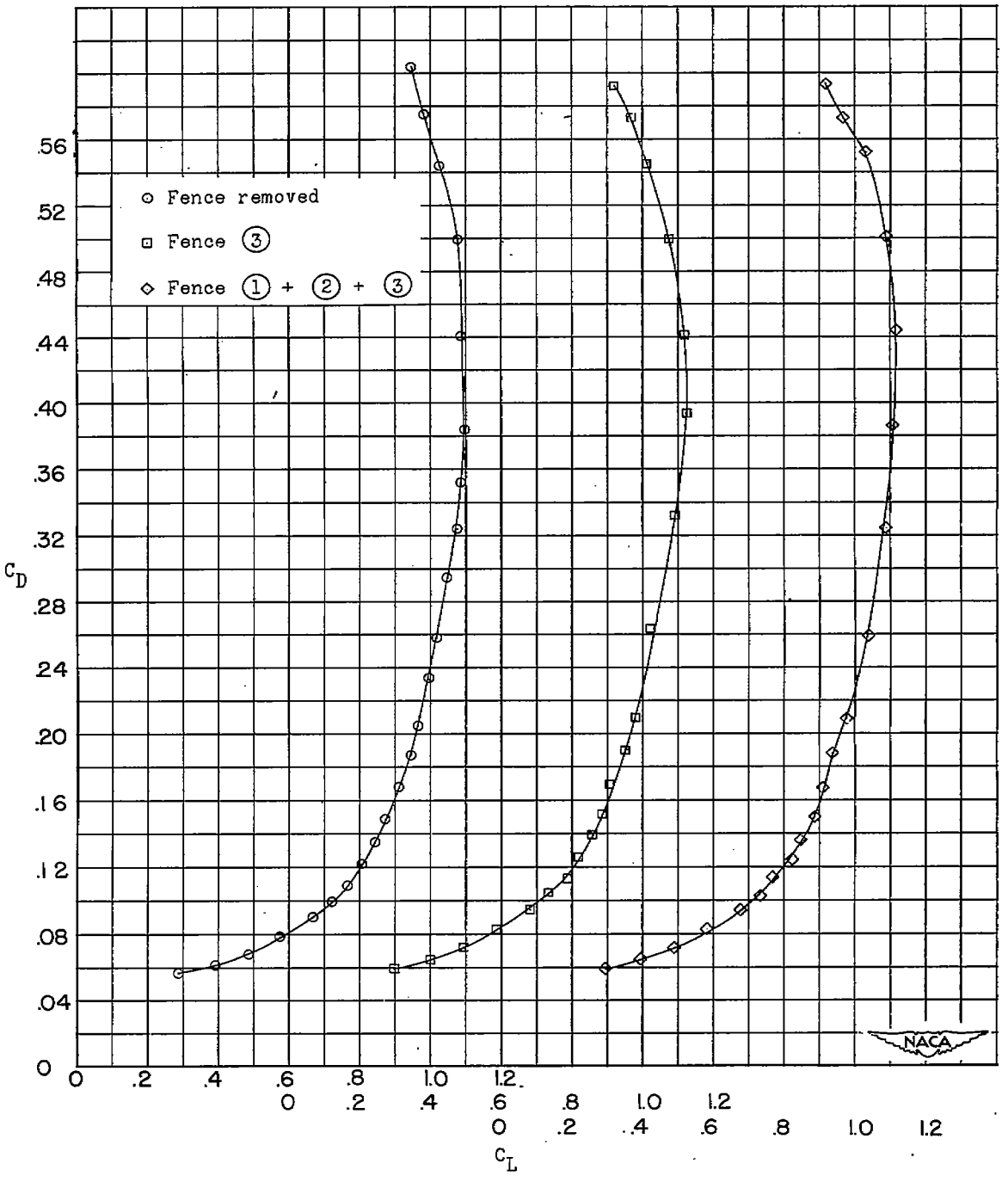

(c) Drag.

Figure 10.- Concluded.

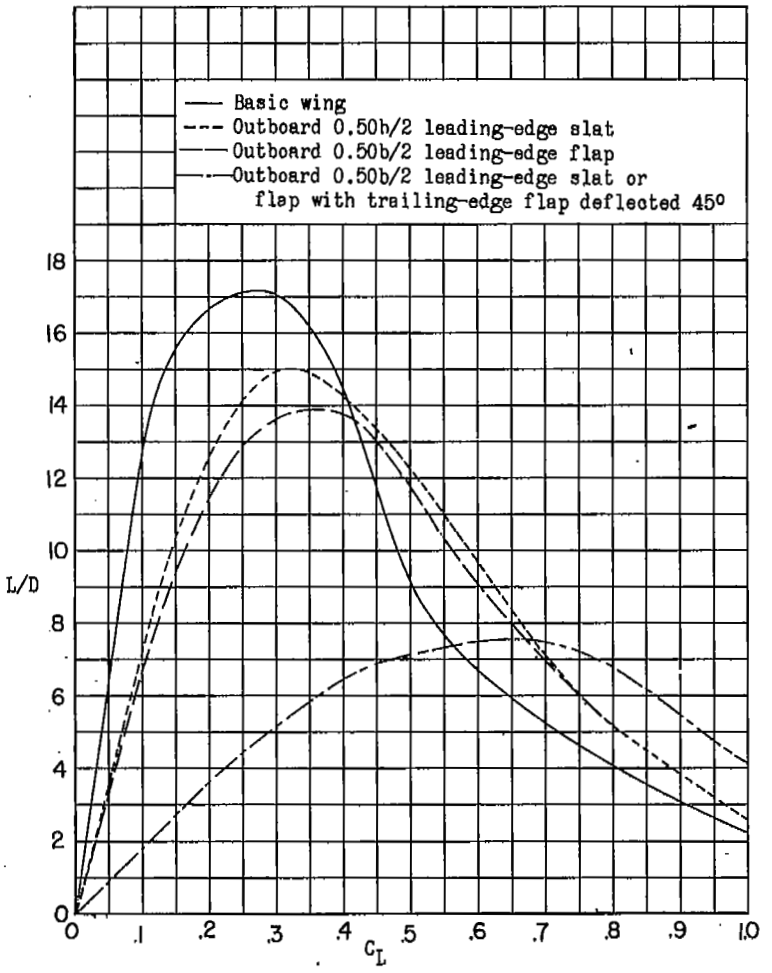

(a) Leading-edge devices.

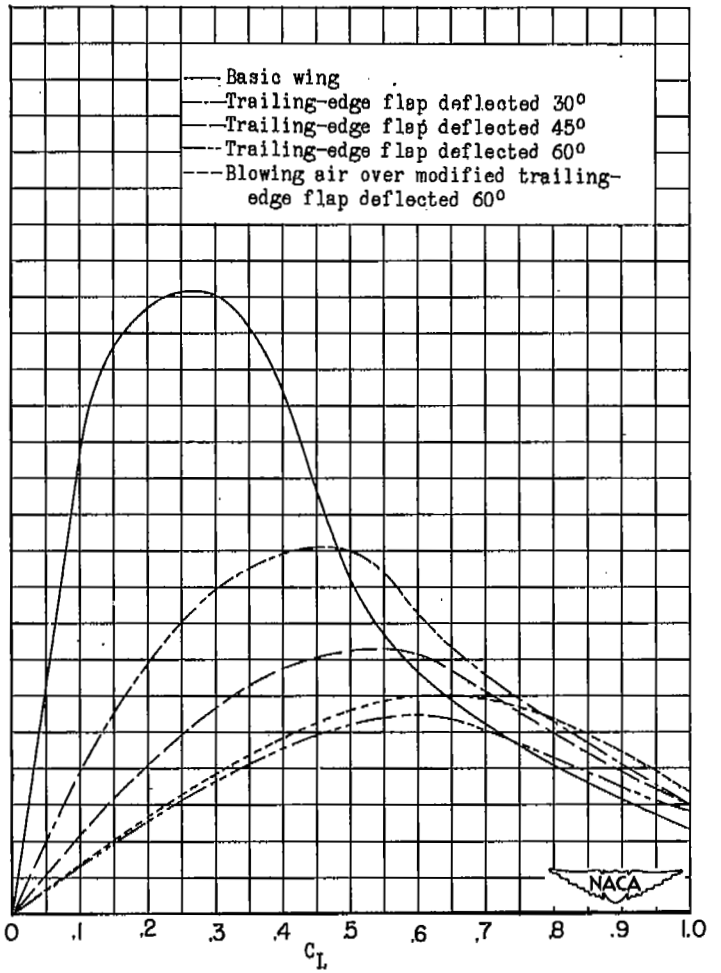

(b) Trailing-edge flap.

Figure 11.- Lift-drag ratios for several configurations tested on a semispan 49.1° sweptback wing.

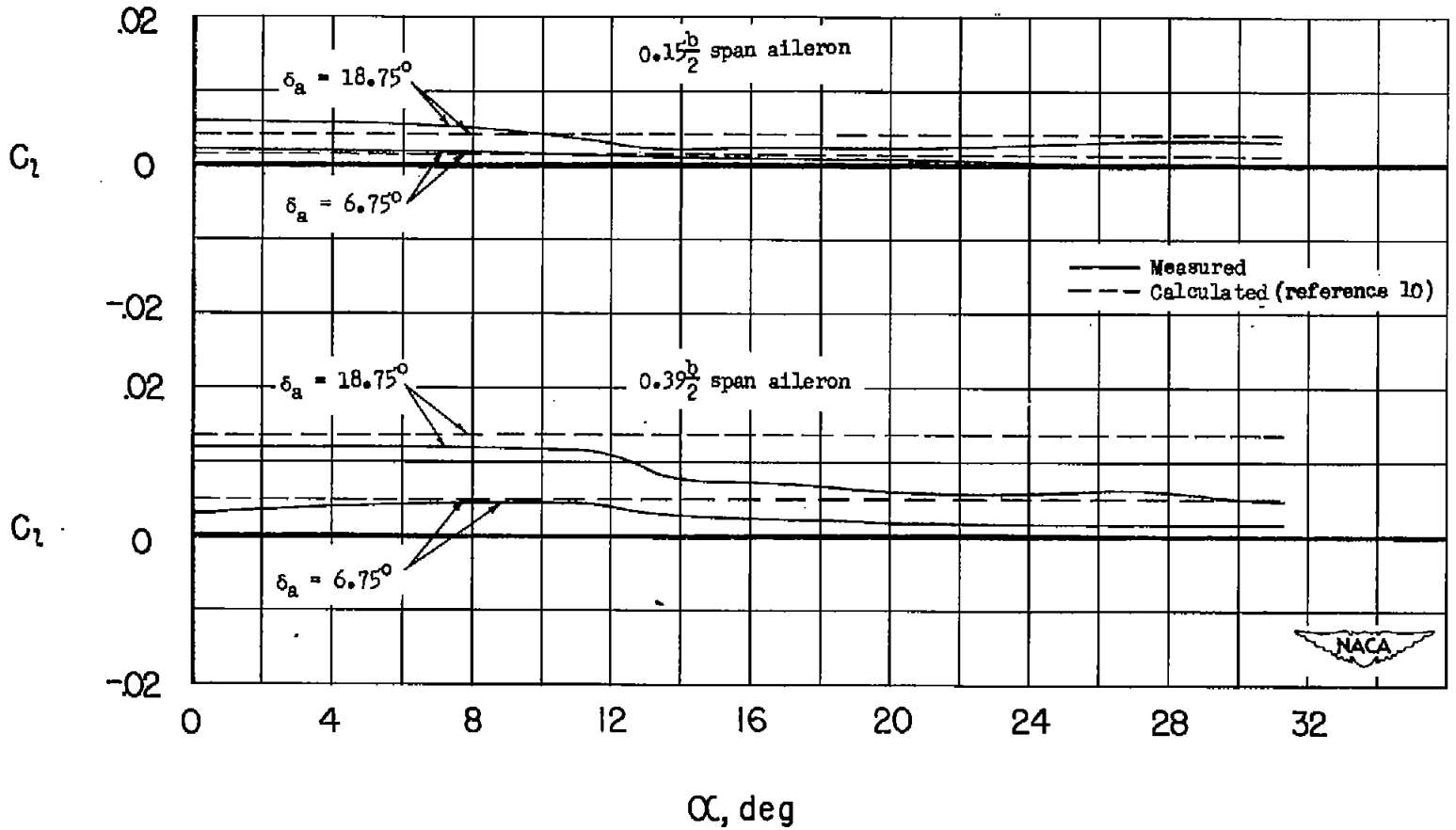

Figure 12.- Rolling-moment characteristics due to aileron deflection for a 49.1° sweptback wing. Basic configuration.

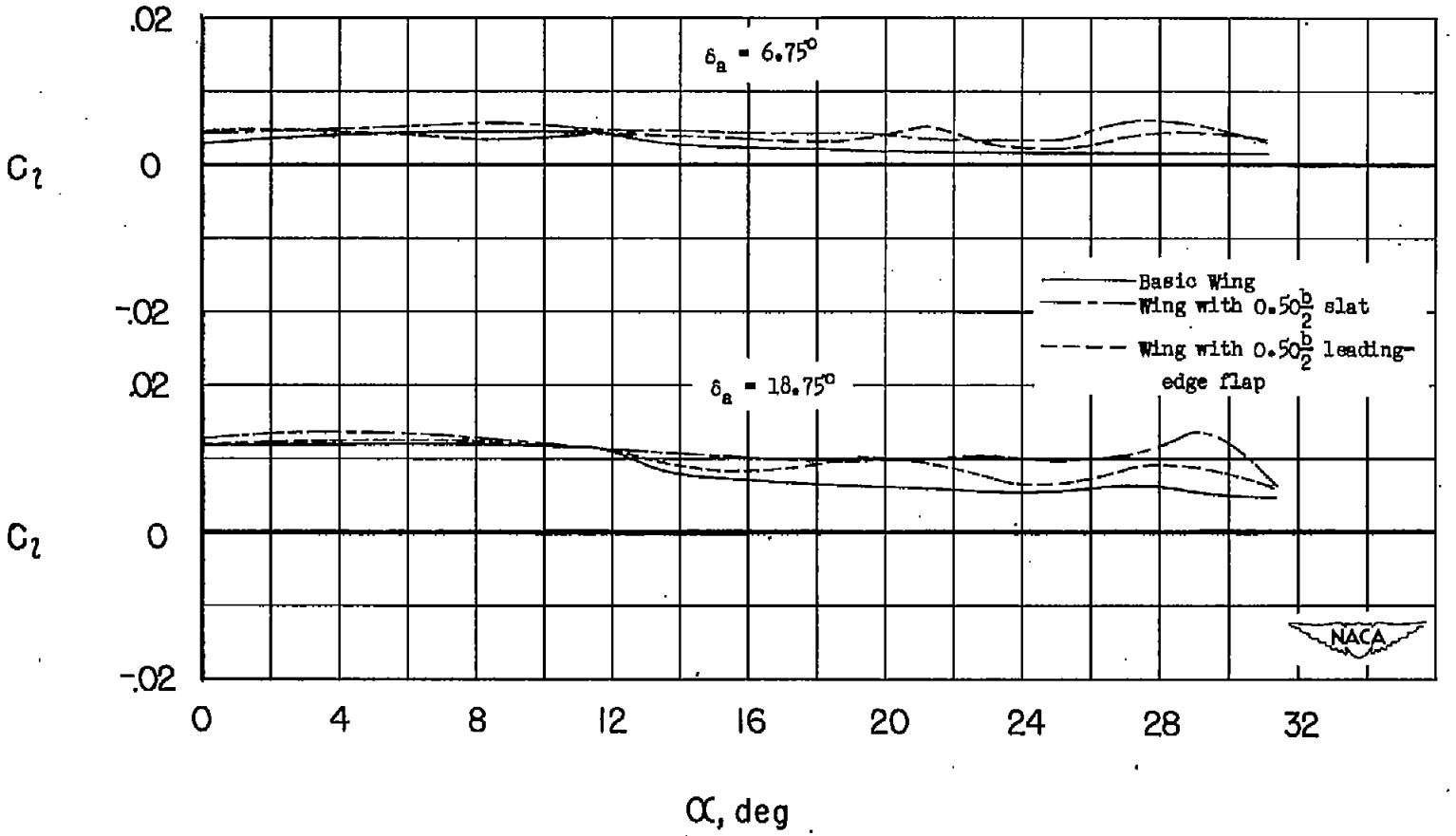

Figure 13.- Effect of 0.50b/2 leading-edge flap and slat on the rolling-moment characteristics due to 0.39b/2 aileron deflection for a 49.1° sweptback wing.

[redacted]

[redacted]